Production cross sections of ^{68}Ga and radioactive by-products in deuteron-induced reactions on natural zinc

Zolbadral Tsoodol[a,b*], Masayuki Aikawa[a,c], Ichinkhorloo Dagvadorj [b,c], Tegshjargal Khishigjargal[d], Namsrai Javkhlantugs[d,1], Yukiko Komori[e], Hiromitsu Haba[e]

[a] *Graduate School of Biomedical Science and Engineering, Hokkaido University, Sapporo 060-8638, Japan*

[b] *Nuclear Research Center, National University of Mongolia, Ulaanbaatar 13330, Mongolia*

[c] *Faculty of Science, Hokkaido University, Sapporo 060-0810, Japan*

[d] *School of Engineering and Applied Sciences, National University of Mongolia, Ulaanbaatar 14201, Mongolia*

[e] *Nishina Center for Accelerator-Based Science, RIKEN, Wako 351-0198, Japan*

Activation cross sections of the deuteron-induced reactions on natural zinc are studied for the production of the medical radionuclide ^{68}Ga. The stacked foil activation method and the γ-ray spectrometry were used. Co-produced radionuclides ^{65,66,67}Ga, ^{63,65,69m}Zn, ^{61}Cu, and ^{58}Co are also investigated to evaluate amounts of impurities for practical use of ^{68}Ga. Physical yields of the radionuclides were deduced from the measured cross sections.

Keyword

Gallium-68; Deuteron irradiation; Zinc target; Excitation function; Cross section; Physical yield

* Corresponding author at Graduate School of Biomedical Science and Engineering, Hokkaido University, Sapporo 060-8638, Japan.
E-mail address: zolbadral@nds.sci.hokudai.ac.jp (Z.Tsoodol).

[1] Deceased

1. Introduction

Gallium-68 ($T_{1/2}$ = 67.71 min) is a positron emitter ($E_{\beta^+}^{mean}$ = 829.5 keV, $I_{\beta^+}^{total}$ = 88.9%) (National Nuclear Data Center, 2017), and is useful for positron emission tomography (PET) (Banerjee and Pomper, 2013). Gallium-68 has the advantages of high sensitivity and resolution, repetitive examinations, and low radiation dose to patients (Velikyan, 2018).

There are practically two methods for ^{68}Ga production for nuclear medicine. The first method is the ^{68}Ge/^{68}Ga generator without cyclotrons co-located at hospitals. However, the parent radionuclide, ^{68}Ge ($T_{1/2}$ = 270.93 days) is cost-ineffective and unable to satisfy the increasing demand for ^{68}Ga in the future (International Atomic Energy Agency, 2019) The second method is the cyclotron production, which is an alternative way for large scale production of ^{68}Ga. The proton-induced reaction on enriched ^{68}Zn is preferable to produce ^{68}Ga with small cyclotrons (e.g., Szelecsényi et al., 2012 and Lin et al., 2018; Riga et al., 2018). The deuteron-induced reactions on zinc are another candidate route for the ^{68}Ga production because the cross sections of the deuteron-induced reactions on zinc isotopes are comparable with those of the proton-induced ones according to the TENDL-2017 library (Koning et al., 2019). A few experimental cross section data of the ^{nat}Zn(d,x)^{68}Ga reaction (Nassiff and Münzel, 1973; Šimečková et al., 2017) and the ^{68}Zn(d,2n)^{68}Ga reaction (Gilly et al., 1963) were reported in the literature. From the comparison of these results, however, a notable discrepancy among them is seen. Therefore, it is necessary to measure the reliable data of the cross sections to investigate the production route. In this paper, we measured the production cross sections of ^{68}Ga and the radioactive by-products via deuteron-induced reactions on natural zinc. Their physical yields were also deduced from the measured cross sections.

2. Experimental methods

The experiment was performed at the AVF cyclotron of the RIKEN RI Beam Factory. The stacked-foil activation technique and the high-resolution γ-ray spectrometry were used to derive the production cross sections.

The stacked target consisted of pure metallic foils of ^{nat}Zn (99.9% purity, Nilaco Corp., Japan) and ^{nat}Ti (99.6% purity, Nilaco Corp., Japan). The isotopic composition of natural zinc was ^{64}Zn: 49.17%, ^{66}Zn: 27.73%, ^{67}Zn: 4.04%, ^{68}Zn: 18.45%, and ^{70}Zn: 0.61%. The size and weight of the ^{nat}Zn and ^{nat}Ti foils were measured to determine the thicknesses of 17.64 mg/cm^2 and 9.31 mg/cm^2, respectively. The foils were cut into 10×10 mm^2 to fit a target holder served as a Faraday cup. Eleven sets of the Zn-Zn-Ti-Ti foils were stacked as the target. Every second foil of Zn and Ti were measured to compensate recoil losses of the products.

The target was irradiated for 22 min by a 23.9-MeV deuteron beam with an avarage intensity of 96

nA. The incident beam energy was measured by the time-of-flight method (Watanabe et al., 2014). The uncertainty of the energy was estimated as ±0.1 MeV. The energy degradation and the uncertainty propagation along the stacked foils were calculated by the SRIM code (Ziegler et al., 2008). The intensity was measured by the Faraday cup.

The γ-ray spectra of the irradiated foils were measured by a high-resolution HPGe detector (ORTEC GMX30P4-70) without chemical separation. The detector was calibrated by a multiple γ-ray point source containing ^{57,60}Co, ^{88}Y, ^{109}Cd, ^{113}Sn ^{137}Cs, ^{139}Ce, and ^{241}Am. The calibration source was bought from Eckert & Ziegler and certified with an uncertainty of 2.3-3.2%. The measured γ-ray spectra were analyzed by the Gamma Studio software (SEIKO EG&G). Each foil was measured five times at maximum after cooling times of 40 min to 18 d to cover different half-lives of products. The distance between the detector and the foils was chosen to keep the dead time less than 7%. The nuclear reaction and decay data for the γ-ray spectrometry were taken from NuDat 2.7 (National Nuclear Data Center, 2017), LiveChart (International Atomic Energy Agency, 2009) and QCalc (Pritychenko and Sonzongni, 2003), and they are summarized in Table 1. All contributing reactions for the formation of the investigated radionuclides are also listed in Table 1.

The cross sections of the ^{nat}Ti(d,x)^{48}V monitor reaction were used to assess the beam parameters. The cross sections were derived from measurements of the 983.5-keV γ-rays (I_γ = 99.98%) emitted from the ^{48}V decay ($T_{1/2}$ = 15.9735 d). The result was compared with the IAEA recommended values (Hermanne et al., 2018). The derived excitation function of the ^{nat}Ti(d,x)^{48}V reaction could be corrected using the beam intensity increased by 6.6% from the measured value by the Faraday cup. The corrected excitation function of the monitor reaction is presented in Fig. 1. This corrected beam intensity (102 nA) was adopted in the estimation of cross sections.

The estimated uncertainty on the beam energy of ± 0.1 MeV in the first foil is propagated to ± 0.9 MeV in the last foil of the stack.

The total uncertainty of the cross sections was 10.0-32.1%. It was estimated as the square root of the quadratic summation of the propagating components; the beam intensity (7%), target thickness (2%), target purity (1%), detector efficiency (6%), γ-intensity (<13%), γ-ray counting (0.5-30.5%), half-life (<5.6%), and peak fitting (3%).

3. Results and discussion

The production cross sections of ^{65,66,67,68}Ga, ^{63,65,69m}Zn, ^{61}Cu, and ^{58}Co were determined and summarized in Table 2. The results compared with previous experimental data available in the EXFOR Library (Otuka et al., 2014) and with theoretical estimation of TENDL-2017 (Koning et al., 2019) are shown in Figs. 2-10. The cross section values extracted from TENDL-2017 and the previous measured data on enriched zinc targets were normalized using the isotopic abundance of natural zinc. Physical yields of the radionuclides were derived from the measured cross sections and shown in Figs. 11-17.

3.1 Production cross sections

3.1.1 The ^{nat}Zn(d,x)^{68}Ga reaction

The cross sections of the ^{nat}Zn(d,x)^{68}Ga reaction were derived from the measurement of 1077.34-keV γ-line (I_γ = 3.22%) from the ^{68}Ga decay ($T_{1/2}$ = 67.71 min). The measured excitation function is shown in Fig. 2 in comparison with the previous experimental data on ^{nat}Zn (Nassiff and Münzel, 1972; Šimečková et al., 2017) and ^{68}Zn (Gilly et al., 1963) and the TENDL-2017 data (Koning et al., 2019). Our result is consistent with the recent data reported by Šimečková et al. (2017) but inconsistent with the data by Nassiff and Münzel (1972) in the whole energy region. The TENDL-2017 data overestimate the most experimental data. Based on the TENDL-2017 prediction, the main contribution comes from the (d,2n) reaction on ^{68}Zn above 6 MeV. The contribution from the (d,n) reaction on ^{67}Zn above 6 MeV is expected to be small. Thus, the normalized data of the (d,2n) reaction on ^{68}Zn (Gilly et al., 1963) are reasonably consistent with the present results on ^{nat}Zn.

3.1.2 The ^{nat}Zn(d,x)^{67}Ga reaction

The 300.217-keV γ-line (I_γ = 16.64%) of ^{67}Ga was used to derive the production cross sections of the ^{nat}Zn(d,x)^{67}Ga reaction. The contribution of the 300.219-keV γ-line (I_γ = 0.797%) of ^{67}Cu was found to be negligible based on its more intense γ line at 184.576 keV (I_γ = 48.7%). The measured excitation function was shown in Fig. 3 in comparison with the experimental data on ^{nat}Zn (Bonardi et al., 2003; Fateh et al., 1996; Khandaker et al., 2015; Nassiff and Münzel, 1972; Šimečková et al., 2017; Tárkányi et al., 2004) and ^{66}Zn (Nassiff and Münzel, 1973; Williams and Irvine, 1963) and the TENDL-2017 data (Koning et al., 2019).

Among the previous data on natural zinc targets, the present result agrees well with the data of Bonardi et al. (2003), Khandaker et al. (2015) and Šimečková et al. (2017). The data reported by Tárkányi et al. (2004) are slightly lower than ours in the higher energy region. The data of Nassiff and Münzel (1972) show lower values while the data reported by Fateh et al. (1996) is much higher than the other experimental data. Based on the TENDL-2017 prediction, the main contribution to the first peak around 8 MeV comes from the (d,n) reaction on ^{66}Zn. The normalized data of the ^{66}Zn(d,n)^{67}Ga reaction by Williams and Irvine (1963) are in good agreement with our data, while the normalized data on ^{66}Zn by Nassiff and Münzel (1973) are inconsistent. The TENDL-2017 data agree with our result up to 17 MeV. Above 17 MeV, the data show higher values than the present data probably due to overestimation of the ^{68}Zn(d,3n) reaction (E_{thr} = 16.4 MeV).

3.1.3 The ^{nat}Zn(d,x)^{66}Ga reaction

The cross sections of the ^{nat}Zn(d,x)^{66}Ga reaction were derived from the measurement of the 1039.22-keV γ-line (I_γ = 37%) of ^{66}Ga. The present result is shown in Fig. 4 with the experimental data studied earlier on ^{nat}Zn (Bonardi et al., 2003; Fateh et al., 1996; Khandaker et al., 2015; Nassiff and Münzel, 1972; Šimečková et al., 2017; Tárkányi et al., 2004) and ^{66}Zn (Bissem et al., 1980; Gilly et al., 1963; Steyn and Meyer, 1973; Vlasov et al., 1957; Williams and Irvine, 1963) and the TENDL-2017 data (Koning et al., 2019).

The present result is consistent with the data studied on ^{nat}Zn by Khandaker et al. (2015), Tárkányi et al. (2004) and Bonardi et al. (2003). The recent data of Šimečková et al. (2017) are slightly higher than our result. The data of Fateh et al. (1996) and Nassiff and Münzel (1972) are entirely inconsistent with the other data. The ^{66}Zn(d,2n)^{66}Ga reaction (E_{thr} = 8.4 MeV) is expected to be dominant in the region up to 20 MeV. The normalized data on ^{66}Zn can be compared with our data in the region. The data reported by Steyn and Meyer (1973) agree well with our measured excitation function. The data by Gilly et al. (1963) and Vlasov et al. (1957) are higher than our data. The data reported by Williams and Irvine (1963) show much higher values around the peak region. In the region above 16 MeV, the data reported by Bissem et al. (1980) show lower values than ours probably due to the lack of the contribution from the (d,3n) reaction on ^{67}Zn (E_{thr} = 15.7 MeV). The peak amplitude is consistent with the TENDL-2017 data, though the position slightly shifts to the lower energy.

3.1.4 The $^{nat}Zn(d,x)^{65}Ga$ reaction

The 115.09-keV γ-line (I_γ=54%) of the radionuclide ^{65}Ga was used to derive the cross sections of the $^{nat}Zn(d,x)^{65}Ga$ reaction. The self-absorption of the γ-line was calculated as 0.4% and found to be negligibly small.

The measured excitation function is shown in Fig. 5 together with the previous experimental data on ^{64}Zn (Bissem et al., 1980; Coetzee and Peisach, 1972; Morrison and Porile, 1959) and on ^{nat}Zn (Nassiff and Münzel, 1972; Šimečková et al., 2017) and the TENDL-2017 data (Koning et al., 2019). Our data have a larger uncertainty than the others due to the relative uncertainty of the intensity (24%) of the 115.09-keV γ-line (International Atomic Energy Agency, 2009). In addition, the uncertainty of the half-life (1.3%) causes the uncertainty of 1.8-5.6% in cross sections and increases the total uncertainty by 0.1-0.6%.

The present result shows an overall agreement with the data of Šimečková et al. (2017) while it disagrees with the data reported by Nassiff and Münzel (1972). Only the (d,n) reaction on ^{64}Zn produces ^{65}Ga below the threshold of the (d,3n) reaction on ^{66}Zn (E_{thr} = 17.8 MeV). Morrison and Porile (1959) reported one cross section of the $^{64}Zn(d,n)^{65}Ga$ reaction at 10.6 MeV, of which data is comparable with our data. The normalized data of the $^{64}Zn(d,n)^{65}Ga$ reaction reported by Bissem et al. (1980) is slightly lower than the present data. The peak amplitude of the TENDL-2017 data agrees with our data within the uncertainty, however the peak position slightly shifts to the lower energy.

3.1.5 The ^{nat}Zn(d,x)^{69m}Zn reaction

The cross sections of the ^{nat}Zn(d,x)^{69m}Zn reaction were derived from the measurement of the 438.63-keV γ-line (I_γ = 94.85%) emitted from the meta-stable state ($T_{1/2}$ = 13.8 h) of the radionuclide ^{69}Zn. The measured excitation function is shown in Fig. 6 in comparison with the previous experimental data on ^{68}Zn (Baron and Cohen, 1963; Gilly et al., 1963), on ^{nat}Zn (Bonardi et al., 2003; Khandaker et al., 2015; Nassiff and Münzel, 1972; Šimečková et al., 2017; Tárkányi et al., 2004), and the TENDL-2017 data (Koning et al., 2019).

The present data are in an overall agreement with the data of Bonardi et al. (2003), Khandaker et al. (2015), Šimečková et al. (2017), and Tárkányi et al. (2004). The data reported by Nassiff and Münzel (1972) are much higher than the other experimental data. Based on the TENDLE-2017 prediction, the (d,p) reaction on ^{68}Zn gives the main contribution in our experimental energy region. Among the data using the enriched ^{68}Zn targets, the data of Gilly et al. (1963) completely disagree with our data. The data reported by Baron and Cohen (1963) at 18 MeV is slightly lower than ours. The TENDL-2017 data underestimate all the experimental data.

3.1.6 The ^{nat}Zn(d,x)^{65}Zn reaction

In addition to the direct reactions, ^{65}Zn ($T_{1/2}$ = 243.93 d) can be produced from the decay of ^{65}Ga ($T_{1/2}$ = 15.2 min). The measured cross sections are cumulative ones because the cooling time was around 18 days. The cross sections were derived from the measurement of 1115.59-keV γ-line (I_γ = 50.04%) of ^{65}Zn and shown in Fig. 7. The result is compared with the experimental data studied earlier on ^{64}Zn (Bissem et al., 1980; Carver and Jones, 1959; Xiaowu et al., 1966), on ^{nat}Zn(Bonardi et al., 2003; Khandaker et al., 2015; Nassiff and Münzel, 1972; Šimečková et al., 2017; Tárkányi et al., 2004), and the TENDL-2017 data (Koning et al., 2019).

Our result is consistent with the recent data of Bonardi et al. (2003), Khandaker et al. (2015), Šimečková et al. (2017) and Tárkányi et al. (2004) but inconsistent with the data of Nassiff and Münzel (1973) below 20 MeV. The present result agrees with the normalized data on ^{64}Zn reported by Xiaowu et al. (1966). It would indicate that the (d,p) reaction on ^{64}Zn is dominant at the first peak. The data by Bissem et al. (1980) on ^{64}Zn show lower values than our data in the energy region above 15 MeV. This tendency in the higher energy region may be caused by the lack of the contributions from the reactions on ^{66}Zn. The TENDL-2017 data underestimate the contribution of the (d,p) reaction on ^{64}Zn.

3.1.7 The ^{nat}Zn(d,x)^{63}Zn reaction

^{63}Zn ($T_{1/2}$ = 38.5 min) can be produced from direct production of the ^{nat}Zn(d,x)^{63}Zn reaction and the decay of ^{63}Ga ($T_{1/2}$ = 32.4 sec) formed by the ^{64}Zn(d,3n)^{63}Ga reaction (E_{thr} = 21.2 MeV). Therefore, the measured cross sections are cumulative ones. The excitation function of the ^{nat}Zn(d,x)^{63}Zn reaction was derived from the measurement of the 669.62-keV γ-line (I_γ = 8.2%) of the radionuclide ^{63}Zn and shown in Fig. 8 and compared with previous experimental data on ^{64}Zn (Bissem et al., 1980), on ^{nat}Zn (Šimečková et al., 2017), and the TENDL-2017 data (Koning et al., 2019). The present data are consistent with the data of Šimečková et al. (2017). Bissem et al. (1980) reported the cumulative cross section of the (d,x) reactions on ^{64}Zn and their normalized data show slightly lower values than our data. The TENDL-2017 data partially agree with experimental values at around 20 MeV.

3.1.8 The $^{nat}Zn(d,x)^{61}Cu$ reaction

The cross sections of the $^{nat}Zn(d,x)^{61}Cu$ reaction were determined using the 282.96-keV γ-line (I_γ = 12.2%) of ^{61}Cu. The relative uncertainty of the γ-line is 18% (International Atomic Energy Agency, 2009), which is a major source of the total uncertainty of the cross sections. The result is shown in Fig. 9 in comparison with the previous experimental data on ^{64}Zn (Baron and Cohen, 1963; Bissem et al., 1980; Daraban et al., 2008; Williams and Irvine, 1963), on ^{nat}Zn (Bonardi et al., 2003; Šimečková et al., 2017; Tárkányi et al., 2004), and the TENDL-2017 data (Koning et al., 2019).

The present result agrees with the data studied using natural zinc targets by Šimečková et al. (2017), Bonardi et al. (2003), and Tárkányi et al. (2004). The result is also compared with the data studied using enriched ^{64}Zn because only the (d,nα) reaction on ^{64}Zn (E_{thr} = 1.4 MeV) contributes to ^{61}Cu production below the threshold energy of the $^{66}Zn(d,3n\alpha)^{61}Cu$ reaction (E_{thr} = 21.04 MeV). The normalized data of Bissem et al. (1980) and Daraban et al. (2008) show slightly lower values than our data. The normalized data of Baron and Cohen (1963) is too low while those of Williams and Irvine (1963) show higher values than ours. The TENDL-2017 data give lower values than the experimental data.

3.1.9 The $^{nat}Zn(d,x)^{58}Co$ reaction

There is a meta-stable state ($T_{1/2}$ = 9.10 h) of ^{58}Co, which decays to the ground state ($T_{1/2}$ = 70.86 d) during a cooling time of about 18 days. Therefore, the cumulative cross sections of the $^{nat}Zn(d,x)^{58}Co$ reaction were derived from the measurement of the 810.76-keV γ-line (I_γ = 99.45%) of the ground state. The excitation function for the ^{58}Co production is shown in Fig. 10 and compared with the previous experimental data on ^{64}Zn (Bissem et al., 1980), on ^{nat}Zn (Khandaker et al., 2015; Tárkányi et al., 2004), and the TENDL-2017 data (Koning et al., 2019).

The present result agrees with both data of Khandaker et al. (2015) and Tárkányi et al. (2004) on ^{nat}Zn. In our experimental energy region, the (d,2α) reaction on ^{64}Zn (E_{thr} = 0.0 MeV) is dominant. The (d,2n2α) reaction on ^{66}Zn (E_{thr} = 17.4 MeV) can contribute to the ^{58}Co production in higher energy region. The normalized data of the $^{64}Zn(d,2\alpha)^{58}Co$ reaction by Bissem et al. (1980) show lower values than our data probably due to the lack of the contribution from the $^{66}Zn(d,2n2\alpha)$ reaction. The TENDL-2017 data show lower values than all the experimental data.

3.2 Integral Yields

Physical yields (Otuka and Takács, 2015) of $^{65,66,67,68}Ga$, $^{63,65,69m}Zn$, ^{61}Cu and ^{58}Co were deduced from spline fitted curves of the measured excitation functions and stopping powers calculated by the SRIM code (Ziegler et al., 2008). The deduced physical yields are shown in Figs. 11-17 and compared with data available in the EXFOR Library (Otuka et al., 2014). Deviations of our results from some of the experimental data are partly caused by the calculation adopted in this work.

The physical yields of the short-lived radionuclides ^{65}Ga, ^{68}Ga and ^{63}Zn are shown in Fig. 11. There are no experimental data found in our literature survey. The physical yields of ^{65}Ga, ^{68}Ga and ^{63}Zn were reported for the first time.

The physical yield of ^{67}Ga is presented in Fig. 12 in comparison with the previous experimental data (Bonardi et al., 2003; Dmitriev et al., 1991; Krasnov et al., 1972; Steyn and Meyer, 1973). The data by Dmitriev et al. (1991) and Bonardi et al. (2003) show higher values than ours at the higher energy region. Our yield curve shows a partial agreement with the yields reported by Steyn and Meyer (1973). The data by Krasnov et al. (1972) present systematically lower values than our data.

The physical yield of ^{66}Ga is shown in Fig. 13 with the previous experimental data (Bonardi et al., 2003; Dmitriev et al., 1991; Steyn and Meyer, 1973). Our result agrees with the yields reported by Steyn and Meyer (1973). However, the data reported by Dmitriev et al. (1991) and at 19 MeV of Bonardi et al. (2003) show systematically higher values than ours.

The physical yields of ^{69m}Zn, ^{65}Zn, ^{61}Cu and ^{58}Co are shown in Figs. 14-17 in comparison with the previous data at 19 MeV (Bonardi et al., 2003). Our data agree with the previous data except for ^{69m}Zn. The previous data of ^{69m}Zn are higher than ours.

3.3 Comparison of proton- and deuteron-induced reactions

The best production reaction of ^{68}Ga for practical use can be discussed using the physical thick target yields. The yields of ^{68}Ga using two reactions, proton- and deuteron-induced reactions on ^{68}Zn, are compared. The yield using the ^{68}Zn(d,2n)^{68}Ga reaction is deduced from that of the ^{nat}Zn(d,x) ^{68}Ga reaction obtained in section 3.2 and assumption of negligibly small contribution of the ^{67}Zn(d,n)^{68}Ga reaction. The yield of the ^{68}Zn(p,n)^{68}Ga reaction is obtained from the previous study (Szelecsényi et al., 1998). The two yields at the threshold energies of the reactions to produce the radioactive impurity ^{67}Ga were 5.6 and 4.2 GBq/μAh for 12.2-MeV proton- and 14.6-MeV deuteron-induced reactions, respectively. Based on the comparison, the 12.2-MeV proton-induced reaction on enriched ^{68}Zn with chemical separation is probably better to produce ^{68}Ga without radioactive impurity. However, the conclusion can be changed if small amount of ^{67}Ga can be accepted.

Conclusions

The excitation functions for the production of ^{68}Ga and by-products such as ^{65,66,67}Ga, ^{63,65,69m}Zn, ^{61}Cu and ^{58}Co via the deuteron-induced reactions on natural zinc were measured up to 24 MeV. The stacked-foil activation technique and the high-resolution γ-ray spectrometry were used for the cross section measurements. The measured data were compared with previous experimental data and the TENDL-2017 data. The derived excitation function of the ^{nat}Zn(d,x)^{68}Ga reaction is consistent with the data of Šimečková et al. (2017). The measured cross sections of the other investigated radionuclides show also good agreements with the recently reported data. The physical yields deduced from measured cross sections partially agree with the previous data. The data obtained in this work are useful to consider the best reaction to produce ^{68}Ga for practical use.

Acknowledgement

The experiment was carried out at RI Beam Factory operated by RIKEN Nishina Center and CNS, University of Tokyo, Japan. This work is supported by JSPS KAKENHI Grant Number 17K07004. Ts.Z is granted a scholarship by the M-JEED project (Mongolian-Japan Engineering Education Development Program, J11B16).

Declarations of interest

None.

Reference

Banerjee, S.R., Pomper, M.G., 2013. Clinical applications of Gallium-68. Appl. Radiat. Isot. 76, 2–13. https://doi.org/10.1016/j.apradiso.2013.01.039

Baron, N., Cohen, B.L., 1963. Activation Cross-Section Survey of Deuteron-Induced Reactions* 1721, 2636–2642.

Bissem, H.H., Georgi, R., Scobel, W., Ernst, J., Kaba, M., Rao, J.R., Strohe, H., 1980. Entrance and exit channel phenomena in d- and He3-induced preequilibrium decay. Phys. Rev. C 22, 1468–1484. https://doi.org/10.1103/PhysRevC.22.1468

Bonardi, M.L., Groppi, F., Birattari, C., Gini, L., Mainardi, C., Ghioni, A., Menapace, E., Abbas, K., Holzwarth, U., Stroosnijder, M.F., 2003. Thin-target excitation functions and optimization of simultaneous production of NCA copper-64 and gallium-66,67 by deuteron induced nuclear reactions on a natural zinc target. J. Radioanal. Nucl. Chem. 257, 229–241. https://doi.org/10.1023/A:1024703022762

Carver, J.H., Jones, G.A., 1959. Radiative deuteron capture $Zn^{64}(d,\gamma)Ga^{66}$. Nucl. Phys. 11, 400–410. https://doi.org/10.1016/0029-5582(59)90278-0

Coetzee, P.P., Peisach, M., 1972. Activation Cross Sections for Deuteron-Induced Reactions on some Elements of the First Transition Series, up to 5.5 MeV. Radiochim. Acta 17, 1–6. https://doi.org/10.1524/ract.1972.17.1.1

Daraban, L., Abbas, K., Simonelli, F., Adam-Rebeles, R., Gibson, N., 2008. Experimental study of excitation functions for the deuteron induced reactions 64Zn(d,2p)64Cu and 64Zn(d,αn)61Cu using the stacked-foil technique. Appl. Radiat. Isot. 66, 261–264. https://doi.org/10.1016/j.apradiso.2007.09.006

Dmitriev, P.P., Panarin, M.V., Molin, G.A., Dmitrieva, Z.P., 1991. ^{66,67}Ga yields in the reactions $^{66-68}$Zn(d,xn). Sov. Atom. Energy 71, 776–777.

Fateh, B., H. Afarideh, Haji-Saeid, S.M., 1996. Proceedings of the 14th International Conference “Cyclotrons and Their Applications”, 8–13 October 1995, Cape Town, South Africa, Word Scientific, Singapore. p. 553.

Gilly, L.J., Henriet, G.A., Alves, M.P., Capron, P.C., 1963. Absolute cross sections and excitation functions for

(d,p) and (d,2n) reactions on Mn^{55}, Cu^{63}, Cu^{65}, Zn^{66}, and Zn^{68} between 3 and 11.6 MeV. Phys. Rev. 131, 1727–1731. https://doi.org/10.1103/PhysRev.131.1727

Hermanne, A., Ignatyuk, A. V., Capote, R., Carlson, B. V., Engle, J.W., Kellett, M.A., Kibédi, T., Kim, G., Kondev, F.G., Hussain, M., Lebeda, O., Luca, A., Nagai, Y., Naik, H., Nichols, A.L., Nortier, F.M., Suryanarayana, S. V., Takács, S., Tárkányi, F.T., Verpelli, M., 2018. Reference Cross Sections for Charged-particle Monitor Reactions. Nucl. Data Sheets 148, 338–382. https://doi.org/10.1016/j.nds.2018.02.009

International Atomic Energy Agency, 2019. Gallium-68 Cyclotron Production. IAEA-TECDOC-1863, IAEA, Vienna.

International Atomic Energy Agency, 2009. LiveChart of Nuclides. [WWW Document]. URL https://www-nds.iaea.org/livechart/.

Khandaker, M.U., Haba, H., Murakami, M., Otuka, N., 2015. Production cross-sections of long-lived radionuclides in deuteron-induced reactions on natural zinc up to 23 MeV. Nucl. Inst. Methods Phys. Res. B 346, 8–16. https://doi.org/10.1016/j.nimb.2015.01.011

Koning, A.J., Rochman, D., Sublet, J.C., Dzysiuk, N., Fleming, M., van der Marck, S., 2019. TENDL: Complete Nuclear Data Library for Innovative Nuclear Science and Technology. Nucl. Data Sheets 155, 1–55. https://doi.org/10.1016/j.nds.2019.01.002

Konstantinov, I.O., 1997. The thin layer activation method and its applications in industry. IAEA-TECDOC-924, IAEA, 43.

Krasnov, N.N., Konstantinov, I.O., Tuev, V.M., Dmitriev, P.P., Konyahin, N.A., 1972. Yield of Ga-67 produced by a cyclotron. Izot. v SSSR 11.

Lin, M., Waligorski, G.J., Lepera, C.G., 2018. Production of curie quantities of ^{68}Ga with a medical cyclotron via the $^{68}Zn(p,n)^{68}Ga$ reaction. Appl. Radiat. Isot. 133, 1–3. https://doi.org/10.1016/j.apradiso.2017.12.010

Morrison, D.L., Porile, N.T., 1959. Absence of Isomerism in Gallium-65. Phys. Rev. 113, 289–290. https://doi.org/10.1103/PhysRev.113.289

Nassiff, S.J., Münzel, H., 1973. Cross sections for the reactions $^{66}Zn(d,n)^{67}Ga$, $^{52}Cr(d,2n)^{52g}Mn$ and $^{186}W(d,2n)^{186}Re$. Radiochim. Acta 19, 97–99.

Nassiff, S.J., Münzel, H., 1972. Excitation functions for deuteron induced reactions on zinc. Radiochem. Radioanal. Lett. 12, 353–361.

National Nuclear Data Center, 2017. Nuclear structure and and decay data on-line library, Nudat 2.7 [WWW Document]. URL https://www.nndc.bnl.gov/nudat2/

Otuka, N., Dupont, E., Semkova, V., Pritychenko, B., Blokhin, A.I., Aikawa, M., Babykina, S., Bossant, M., Chen, G., Dunaeva, S., Forrest, R.A., Fukahori, T., Furutachi, N., Ganesan, S., Ge, Z., Gritzay, O.O., Herman, M., Hlavač, S., Kato, K., Lalremruata, B., Lee, Y.O., Makinaga, A., Matsumoto, K.,

Mikhaylyukova, M., Pikulina, G., Pronyaev, V.G., Saxena, A., Schwerer, O., Simakov, S.P., Soppera, N., Suzuki, R., Takács, S., Tao, X., Taova, S., Tárkányi, F., Varlamov, V. V., Wang, J., Yang, S.C., Zerkin, V., Zhuang, Y., 2014. Towards a More complete and accurate experimental nuclear reaction data library (EXFOR): International collaboration between nuclear reaction data centres (NRDC). Nucl. Data Sheets 120, 272–276. https://doi.org/10.1016/j.nds.2014.07.065

Otuka, N., Takács, S., 2015. Definitions of radioisotope thick target yields. Radiochim. Acta 103, 1–6. https://doi.org/10.1515/ract-2013-2234

Pritychenko, B., Sonzongni, A., 2003. Q-value Calculator (QCalc). [WWW Document]. URL https://www.nndc.bnl.gov/qcalc/

Riga, S., Cicoria, G., Pancaldi, D., Zagni, F., Vichi, S., Dassenno, M., Mora, L., Lodi, F., Morigi, M.P., Marengo, M., 2018. Production of Ga-68 with a General Electric PETtrace cyclotron by liquid target. Phys. Medica 55, 116–126. https://doi.org/10.1016/j.ejmp.2018.10.018

Šimečková, E., Bém, P., Mrázek, J., Štefánik, M., Běhal, R., Gladolev, V., 2017. Proton and deuteron activation measurements at the NPI and future plans in SPIRAL2/NFS. EPJ Web Conf. 146, 11034. https://doi.org/10.1051/epjconf/201714611034

Steyn, J., Meyer, B.., 1973. Production of ^{67}Ga by deuteron bombardment of natural zinc. Int. J. Appl. Radiat. Isot. 24, 369–372.

Szelecsényi, F., Boothe, T.E., Takács, S., Tárkányi, F., Tavano, E., 1998. Evaluated cross section and thick target yield data bases of Zn + p processes for practical applications. Appl. Radiat. Isot. 49, 1005–1032. https://doi.org/10.1016/S0969-8043(97)10103-8

Szelecsényi, F., Kovács, Z., Nagatsu, K., Fukumura, K., Suzuki, K., Mukai, K., 2012. Investigation of direct production of ^{68}Ga with low energy multiparticle accelerator. Radiochim. Acta 100, 5–11. https://doi.org/10.1524/ract.2011.1896

Tárkányi, F., Takács, S., Ditrói, F., Hermanne, A., Sonck, M., Shubin, Y., 2004. Excitation functions of deuteron induced nuclear reactions on natural zinc up to 50 MeV. Nucl. Instruments Methods Phys. Res. Sect. B Beam Interact. with Mater. Atoms 217, 531–550. https://doi.org/10.1016/j.nimb.2003.11.089

Velikyan, I., 2018. Prospective of ^{68}Ga Radionuclide Contribution to the Development of Imaging Agents for Infection and Inflammation. Contrast Media Mol. Imaging 2018, ID 9713691. https://doi.org/10.1155/2018/9713691

Vlasov, N.A., Kalinin, S.P., Ogloblin, A.A., Pankratov, V.M., Rudakov, P., Serikov, I. N. and Sidorov, V.A., 1957. Excitation functions for the reactions Mg-24(d,a)Na-22, Fe-54(d,a)Mn-52, Fe-54(d,n)Co-55, Zn-66(d,2n)Ga-66. At. Energ.2. J. Sov. At. Energy 2, 189.

Watanabe, T., Fujimaki, M., Fukunishi, N., Imao, H., Kamigaito, O., Kase, M., Komiyama, M., Sakamoto, N., Suda, K., Wakasugi, M., Yamada, K., 2014. Beam energy and longitudinal beam profile measurement system at the RIBF, in: Proceedings of the 5th International Particle Accelerator Conference (IPAC 2014).

pp. 3566–3568.

Williams, D.C., Irvine, J.W.J., 1963. Nuclear excitation functions and thick-target yields: Zn+d and Ar^{40}(d,a). Phys. Rev. 130, 265–271.

Xiaowu, C., Zhenxia, W., Wang. Zhenjie, Yang. Jinqing, 1966. Some measurements of deuteron induced excitation function at 13 MeV. Acta Phys. Sin. 22, 250–252.

Ziegler, J.F., Biersack, J.P., Ziegler, M.D., 2008. SRIM: the Stopping and Range of Ions in Matter. [Online]. Available: http://www.srim.org.

Figure captions

Fig. 1. The excitation function of the ^{nat}Ti(d,x)^{48}V monitor reaction compared with the recommended values (Hermanne et al., 2018).

Fig. 2. The excitation function of the ^{nat}Zn(d,x)^{68}Ga reaction. The data on enriched ^{68}Zn are nomalized using the natural isotopic abundance.

Fig. 3. The excitation function of the ^{nat}Zn(d,x)^{67}Ga reaction. The data on enriched ^{66}Zn are nomalized using the natural isotopic abundance.

Fig. 4. The excitation function of the ^{nat}Zn(d,x)^{66}Ga reaction. The data on enriched ^{66}Zn are nomalized using the natural isotopic abundance.

Fig. 5. The excitation function of the ^{nat}Zn(d,x)^{65}Ga reaction. The data on enriched ^{64}Zn are nomalized using the natural isotopic abundance.

Fig. 6. The excitation function of the ^{nat}Zn(d,x)^{69m}Zn reaction. The data on enriched ^{68}Zn are nomalized using the natural isotopic abundance.

Fig. 7. The excitation function of the ^{nat}Zn(d,x)^{65}Zn reaction. The data on enriched ^{64}Zn are nomalized using the natural isotopic abundance.

Fig. 8. The excitation function of the ^{nat}Zn(d,x)^{63}Zn reaction. The data on enriched ^{64}Zn are nomalized using the natural isotopic abundance.

Fig. 9. The excitation function of the ^{nat}Zn(d,x)^{61}Cu reaction. The data on enriched ^{64}Zn are nomalized using the natural isotopic abundance.

Fig. 10. The excitation function of the ^{nat}Zn(d,x)^{58}Co reaction. The data on enriched ^{64}Zn are nomalized using the natural isotopic abundance.

Fig. 11. The physical yields of ^{65}Ga, ^{68}Ga and ^{63}Zn via the deuteron-induced reactions on ^{nat}Zn.

Fig. 12. The physical yield of ^{67}Ga via the deuteron-induced reactions on ^{nat}Zn.

Fig. 13. The physical yield of ^{66}Ga via the deuteron-induced reactions on ^{nat}Zn.

Fig. 14. The physical yield of ^{69m}Zn via the deuteron-induced reactions on ^{nat}Zn.

Fig. 15. The physical yield of ^{65}Zn via the deuteron-induced reactions on ^{nat}Zn.

Fig. 16. The physical yields of ^{61}Cu via the deuteron-induced reactions on ^{nat}Zn.

Fig. 17. The physical yields of ^{58}Co via the deuteron-induced reactions on ^{nat}Zn.

Tables

Table 1
Reactions and decay data for reaction products (International Atomic Energy Agency, 2009; National Nuclear Data Center, 2017; Pritychenko and Sonzongni, 2003)

Nuclide	Half-life	Decay mode (%)	E_γ (keV)	I_γ (%)	Contributing reaction	Q-value (MeV)
^{68}Ga	67.71 min	ε+β^+(100)	**1077.34**	3.22(3)	^{66}Zn(d,γ)	11.3
					^{67}Zn(d,n)	4.3
					^{68}Zn(d,2n)	-5.9
					^{70}Zn(d,4n)	-21.6
^{67}Ga	3.2617 d	ε (100)	91.265	3.11(4)	^{66}Zn(d,n)	3.0
			93.310	38.81(3)	^{67}Zn(d,2n)	-4.0
			184.576	21.41(10)	^{68}Zn(d,3n)	-14.2
			208.950	2.460(10)		
			300.217	16.64(12)		
			393.527	4.56(24)		
^{66}Ga	9.49 h	ε+β^+(100)	833.5324	5.9(3)	^{64}Zn(d,γ)	10.8
			1039.220	37.0(20)	^{66}Zn(d,2n)	-8.2
					^{67}Zn(d,3n)	-15.2
^{65}Ga	15.2 min	ε+β^+(100)	53.93	4.9(10)	^{64}Zn(d,n)	1.7
			61.2	11.4(24)	^{66}Zn(d,3n)	-17.3
			115.09	54(13)		
			153.0	8.9(19)		
			206.9	2.5(5)		
			751.8	8.1(16)		
			768.9	1.3(3)		
			932.2	1.8(4)		
^{69m}Zn	13.756 h	β^- (99.97)	**438.634**	94.85(7)	^{68}Zn(d,p)	4.3
					^{70}Zn(d,t)	-3.0
^{65}Zn	243.93 d	ε+β^+(100)	**1115.539**	50.04(10)	^{64}Zn(d,p)	5.7
					^{66}Zn(d,t)	-4.8
					^{67}Zn(d,p3n)	-20.3
					^{65}Ga decay	
^{63}Zn	38.47 min	ε+β^+(100)	**669.62**	8.2(3)	^{64}Zn(d,t)	-5.6
			962.06	6.5 (4)	^{63}Ga decay	
^{61}Cu	3.339 h	ε+β^+(100)	67.4	4.2(8)	^{64}Zn(d,αn)	-1.4
			282.956	12.2(22)	^{66}Zn(d,α3n)	-20.4
			373.050	2.1(4)		
			588.605	1.17(21)		
			656.008	10.8(20)		
			908.631	1.10(20)		
			1185.234	3.7(7)		
^{58}Co	70.86 d	ε+β^+(100)	**810.7593**	99.450(10)	^{64}Zn(d,2α)	-2.1
					^{66}Zn(d,2n2α)	-16.9
Monitor reaction						
^{48}V	15.9735 d	ε +β^+(100)	944.13	7.870(7)	^{46}Ti(d,γ)	13.5
			983.52	99.98(4)	^{47}Ti(d,n)	4.6
			1312.11	98.2(3)	^{48}Ti(d,2n)	-7.0
					^{49}Ti(d,3n)	-15.2

Table 2

Measured cross sections

Energy (MeV)	Cross sections (mb)								
	^{68}Ga	^{67}Ga	^{66}Ga	^{65}Ga	^{69m}Zn	^{65}Zn	^{63}Zn	^{61}Cu	^{58}Co
23.2 ±0.3	99.5 ±12.8	100.3 ±10.6	100.2 ±11.4	24.5 ±6.4	6.8 ±0.7	175.9 ±17.7	60.9 ±7.2	45.2 ±9.6	4.0 ±0.4
21.9 ±0.3	121.1 ±15.0	87.5 ±9.4	111.7 ±12.7	22.3 ±5.9	7.3 ±0.7	145.5 ±14.6	35.3 ±4.6	53.5 ±11.3	3.3 ±0.4
20.4 ±0.3	130.6 ±16.5	74.2 ±8.2	126.2 ±14.3	22.8 ±6.0	7.8 ±0.8	119.9 ±12.1	23.0 ±3.4	54.7 ±11.6	2.9 ±0.3
18.9 ±0.4	158.2 ±19.1	67.0 ±7.5	136.2 ±15.4	24.6 ±6.6	8.4 ±0.8	112.5 ±11.4	8.3 ±2.1	53.0 ±11.2	2.6 ±0.3
17.3 ±0.4	169.1 ±20.5	57.2 ±6.9	135.6 ±15.4	25.6 ±6.9	9.2 ±0.9	117.8 ±11.9	8.2 ±2.4	45.1 ±9.6	1.8 ±0.2
15.6 ±0.4	178.3 ±21.6	60.2 ±6.7	124.5 ±14.1	30.1 ±8.1	10.6 ±1.1	141.7 ±14.3	5.3 ±2.6	34.4 ±7.4	1.1 ±0.1
13.7 ±0.5	167.2 ±21.2	69.4 ±8.1	100.5 ±11.4	38.4 ±10.4	12.1 ±1.2	174.9 ±17.6		23.6 ±5.3	
11.6 ±0.5	137.2 ±17.5	89.4 ±11.8	51.7 ±5.9	52.5 ±14.2	13.8 ±1.4	228.4 ±23.2		8.1 ±2.0	
9.2 ±0.6	68.8 ±10.7	115.2 ±13.5	2.3 ±0.3	74.9 ±19.9	15.5 ±1.5	299.4 ±30.2			
6.2 ±0.8	12.1 ±3.9	101.5 ±11.9		74.0 ±20.0	11.9 ±1.2	266.0 ±26.9			
2.6 ±0.9		0.23 ±0.05			0.04±0.01				

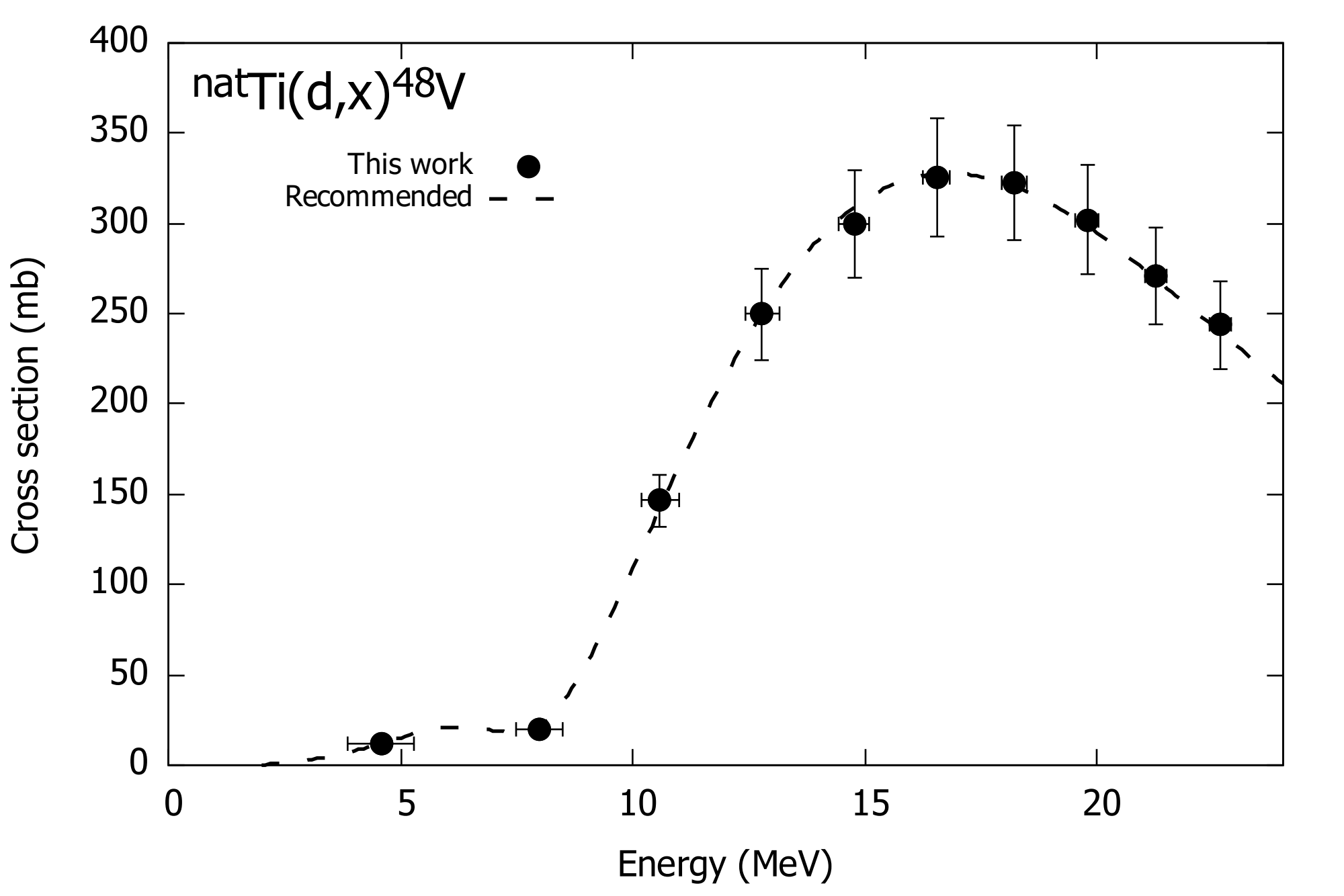
nat Ti(d,x)48V
This work
Recommended
Cross section (mb)
Energy (MeV)
0
50
100
150
200
250
300
350
400
0
5
10
15
20

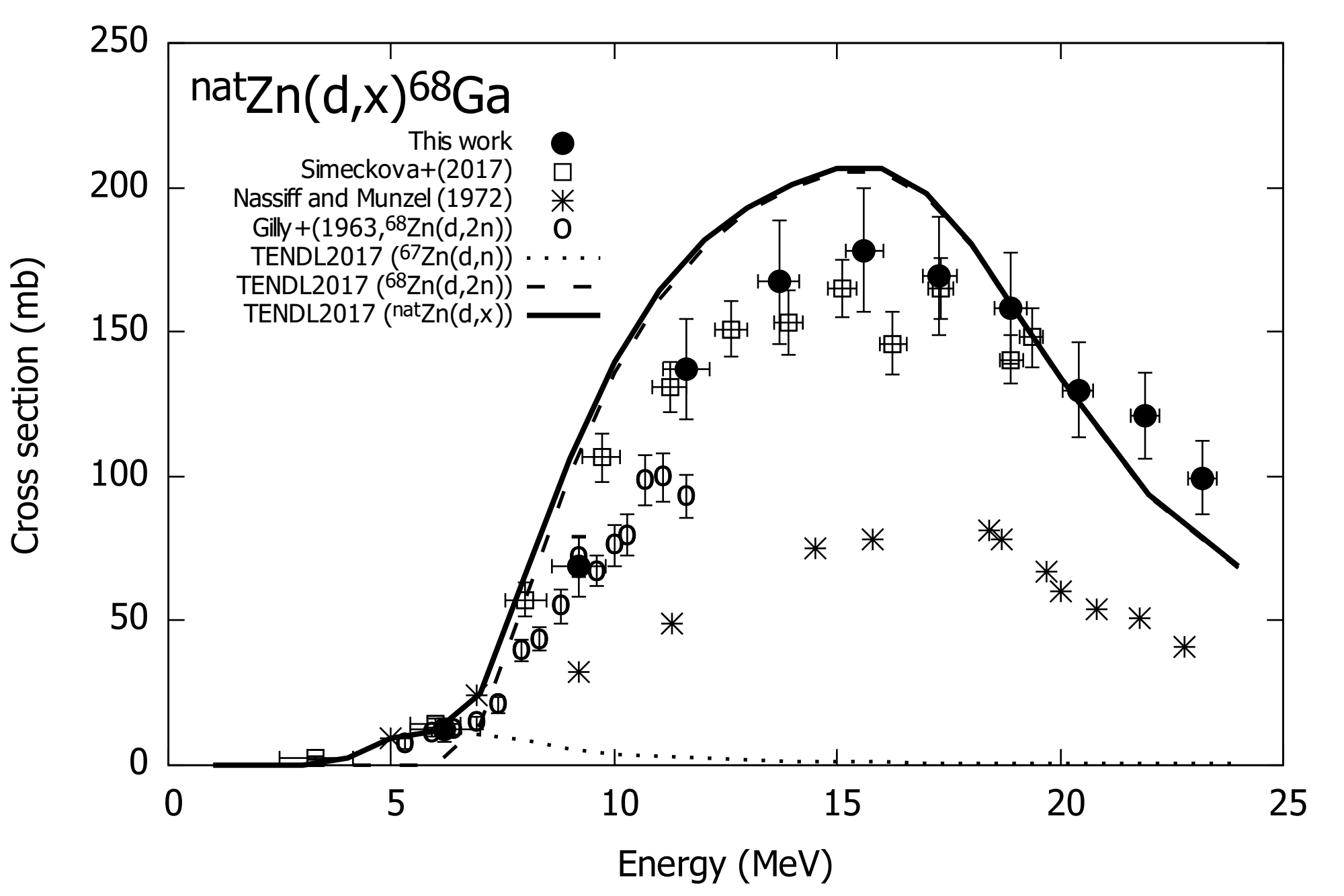
natZn(d,x)68Ga
This work
Simeckova+(2017)
Nassiff and Munzel (1972)
Gilly+(1963,68Zn(d,2n))
TENDL2017 (67Zn(d,n))
TENDL2017 (68Zn(d,2n))
TENDL2017 (natZn(d,x))
Cross section (mb)
Energy (MeV)
0
50
100
150
200
250
0
5
10
15
20
25

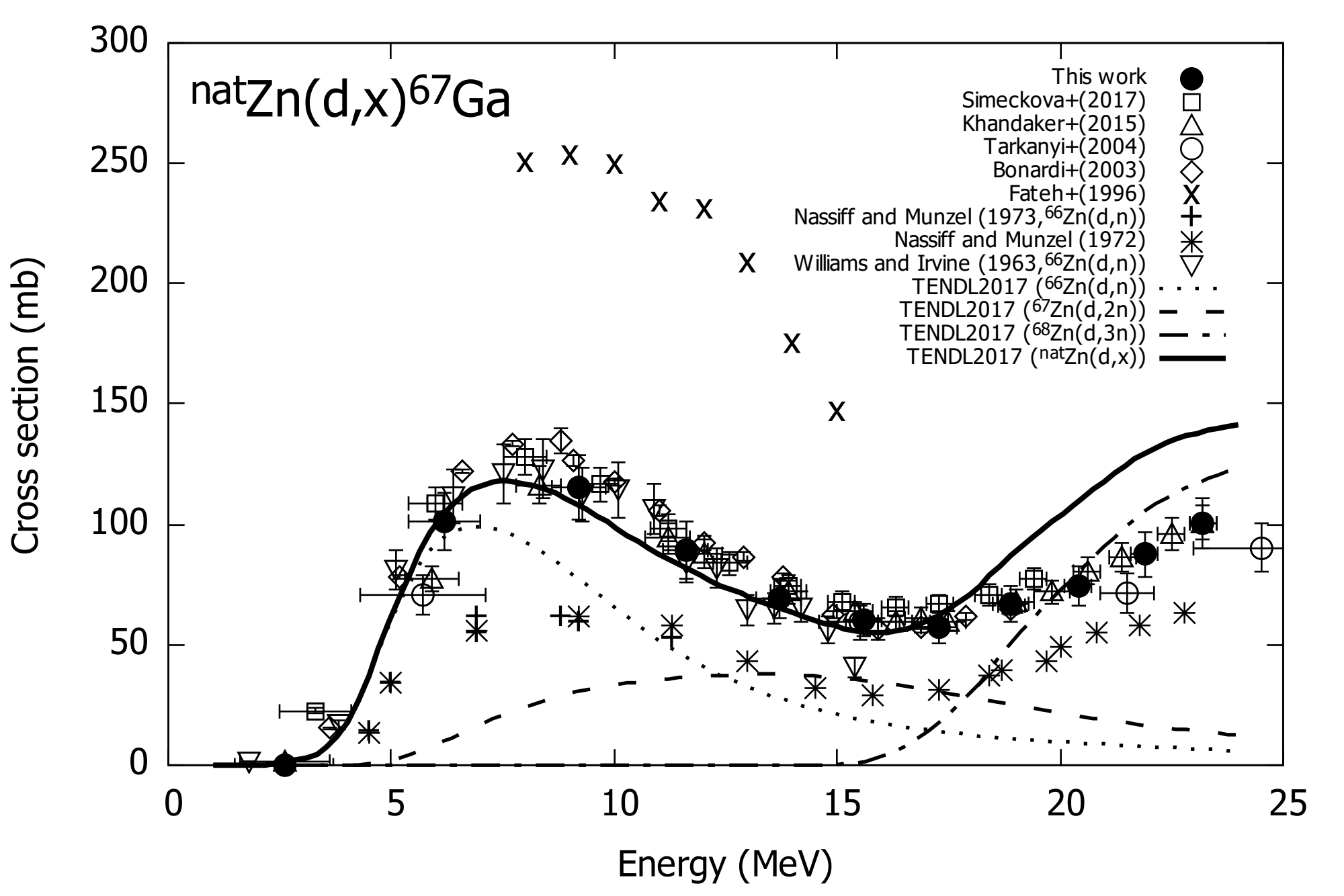
natZn(d,x)67Ga
This work
Simeckova+(2017)
Khandaker+(2015)
Tarkanyi+(2004)
Bonardi+(2003)
Fateh+(1996)
Nassiff and Munzel (1973,66Zn(d,n))
Nassiff and Munzel (1972)
Williams and Irvine (1963,66Zn(d,n))
TENDL2017 (66Zn(d,n))
TENDL2017 (67Zn(d,2n))
TENDL2017 (68Zn(d,3n))
TENDL2017 (natZn(d,x))
Cross section (mb)
Energy (MeV)
0
50
100
150
200
250
300
0
5
10
15
20
25

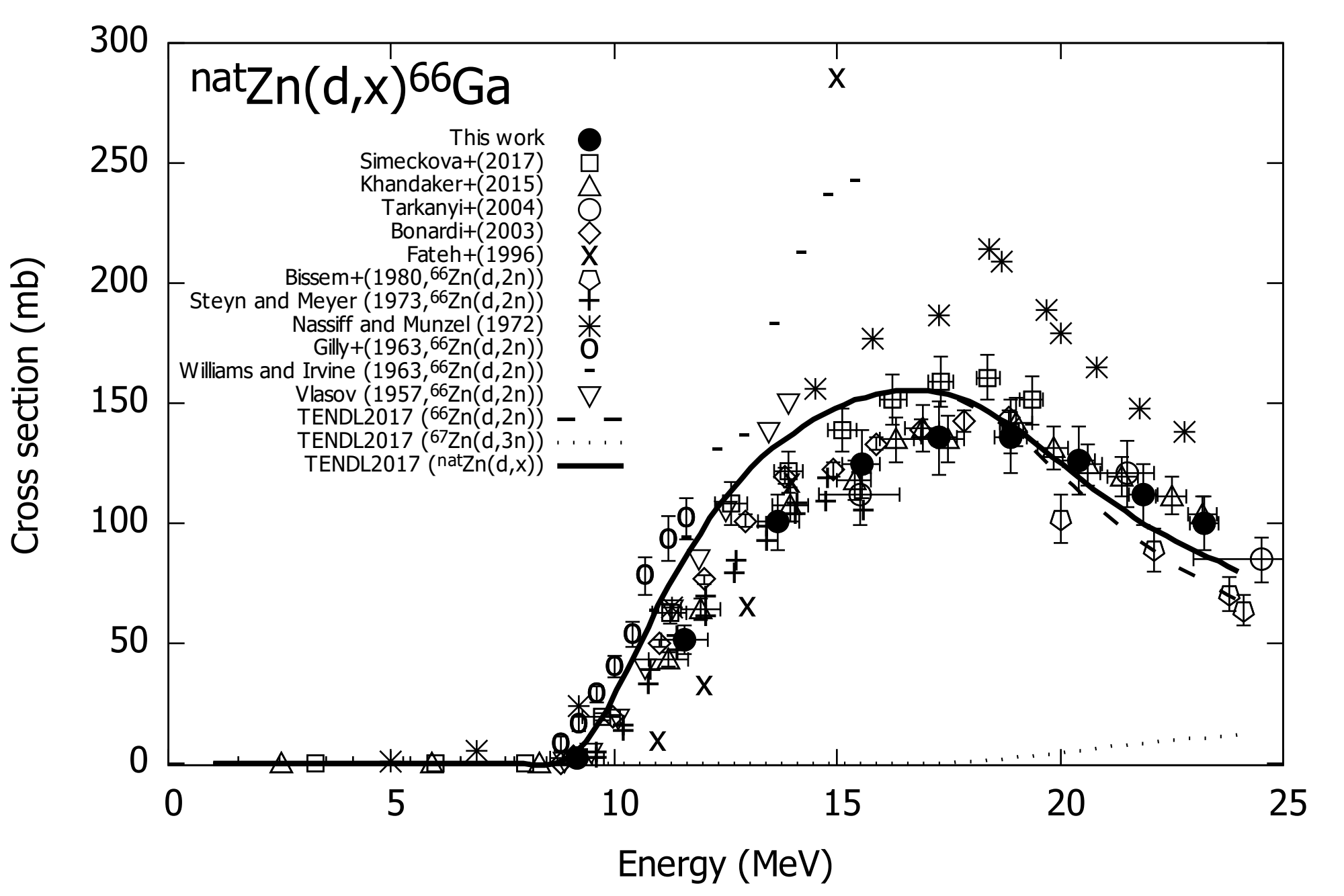
natZn(d,x)66Ga
This work
Simeckova+(2017)
Khandaker+(2015)
Tarkanyi+(2004)
Bonardi+(2003)
Fateh+(1996)
Bissem+(1980,66Zn(d,2n))
Steyn and Meyer (1973,66Zn(d,2n))
Nassiff and Munzel (1972)
Gilly+(1963,66Zn(d,2n))
Williams and Irvine (1963,66Zn(d,2n))
Vlasov (1957,66Zn(d,2n))
TENDL2017 (66Zn(d,2n))
TENDL2017 (67Zn(d,3n))
TENDL2017 (natZn(d,x))
Cross section (mb)
Energy (MeV)
0
50
100
150
200
250
300
0
5
10
15
20
25

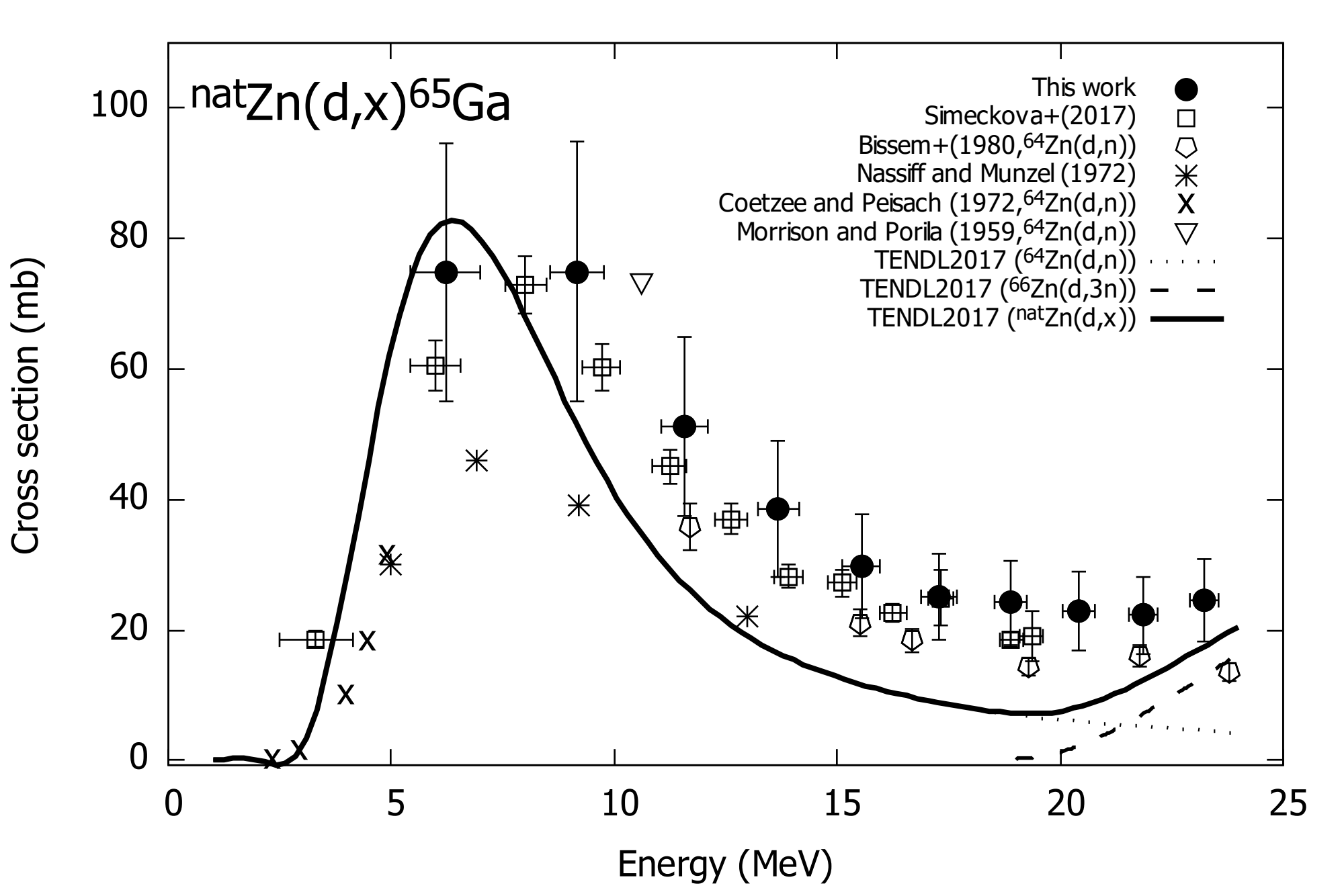
natZn(d,x)65Ga
This work
Simeckova+(2017)
Bissem+(1980,64Zn(d,n))
Nassiff and Munzel (1972)
Coetzee and Peisach (1972,64Zn(d,n))
Morrison and Porila (1959,64Zn(d,n))
TENDL2017 (64Zn(d,n))
TENDL2017 (66Zn(d,3n))
TENDL2017 (natZn(d,x))
Cross section (mb)
Energy (MeV)
0
20
40
60
80
100
0
5
10
15
20
25

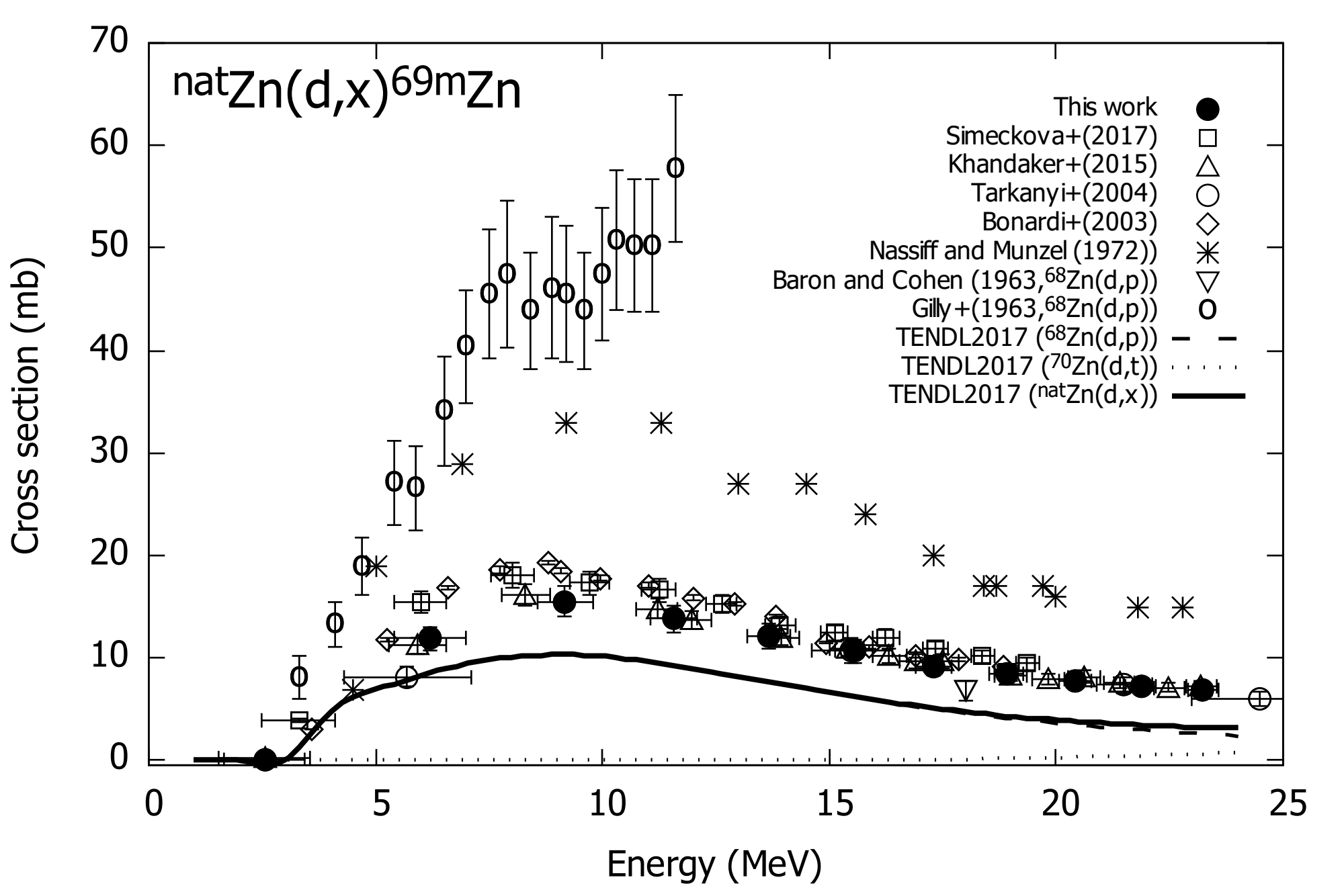
natZn(d,x)69mZn
This work
Simeckova+(2017)
Khandaker+(2015)
Tarkanyi+(2004)
Bonardi+(2003)
Nassiff and Munzel (1972))
Baron and Cohen (1963,68Zn(d,p))
Gilly+(1963,68Zn(d,p))
TENDL2017 (68Zn(d,p))
TENDL2017 (70Zn(d,t))
TENDL2017 (natZn(d,x))
Cross section (mb)
Energy (MeV)
0
10
20
30
40
50
60
70
0
5
10
15
20
25

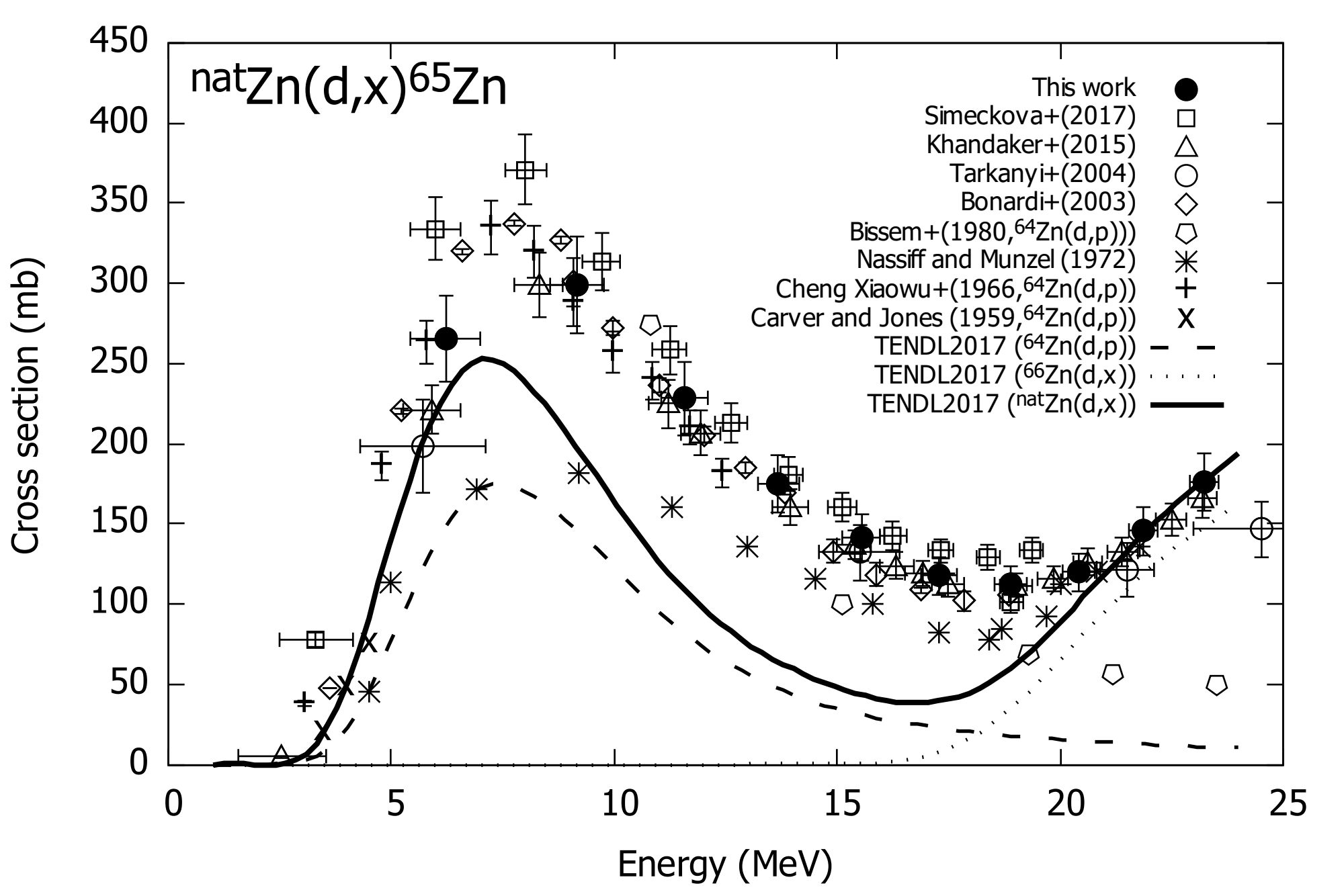
natZn(d,x)65Zn
This work
Simeckova+(2017)
Khandaker+(2015)
Tarkanyi+(2004)
Bonardi+(2003)
Bissem+(1980,64Zn(d,p)))
Nassiff and Munzel (1972)
Cheng Xiaowu+(1966,64Zn(d,p))
Carver and Jones (1959,64Zn(d,p))
TENDL2017 (64Zn(d,p))
TENDL2017 (66Zn(d,x))
TENDL2017 (natZn(d,x))
Cross section (mb)
Energy (MeV)
0
50
100
150
200
250
300
350
400
450
0
5
10
15
20
25

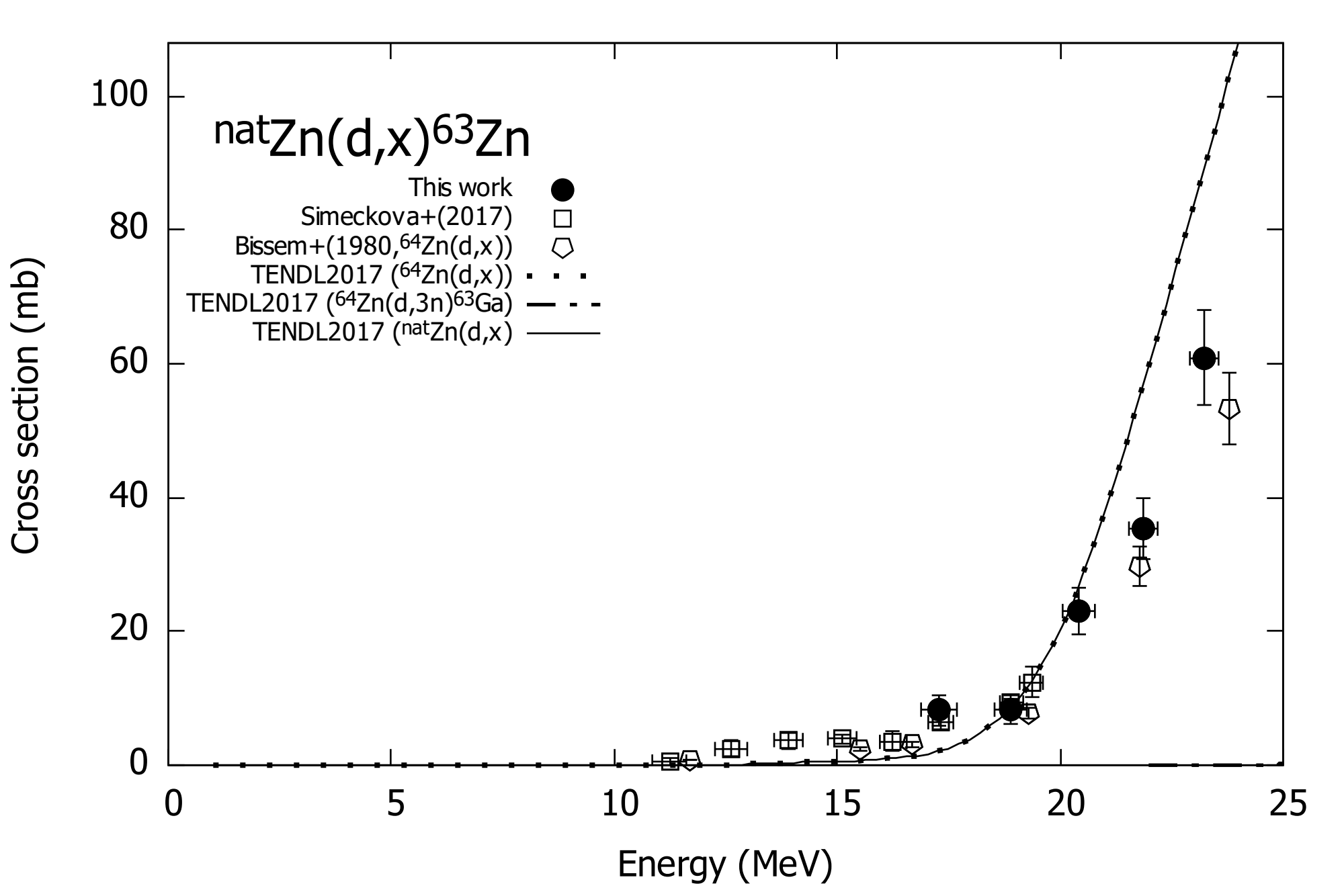
^{nat}Zn(d,x)^{63}Zn
This work
Simeckova+(2017)
Bissem+(1980,^{64}Zn(d,x))
TENDL2017 (^{64}Zn(d,x))
TENDL2017 (^{64}Zn(d,3n)^{63}Ga)
TENDL2017 (^{nat}Zn(d,x)
Cross section (mb)
Energy (MeV)
0
20
40
60
80
100
0
5
10
15
20
25

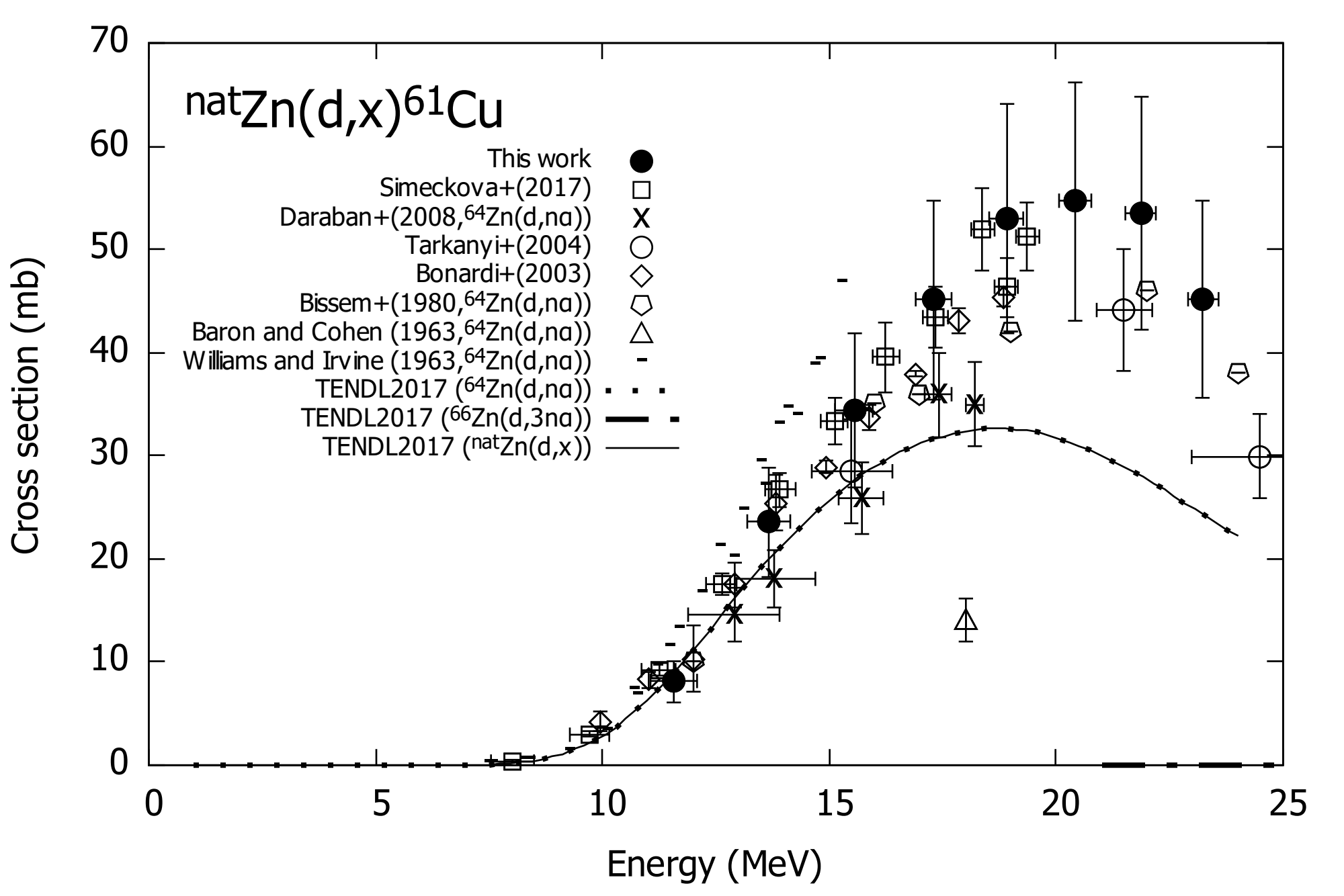
natZn(d,x)61Cu
This work
Simeckova+(2017)
Daraban+(2008,64Zn(d,nα))
Tarkanyi+(2004)
Bonardi+(2003)
Bissem+(1980,64Zn(d,nα))
Baron and Cohen (1963,64Zn(d,nα))
Williams and Irvine (1963,64Zn(d,nα))
TENDL2017 (64Zn(d,nα))
TENDL2017 (66Zn(d,3nα))
TENDL2017 (natZn(d,x))
Cross section (mb)
Energy (MeV)
0
10
20
30
40
50
60
70
0
5
10
15
20
25

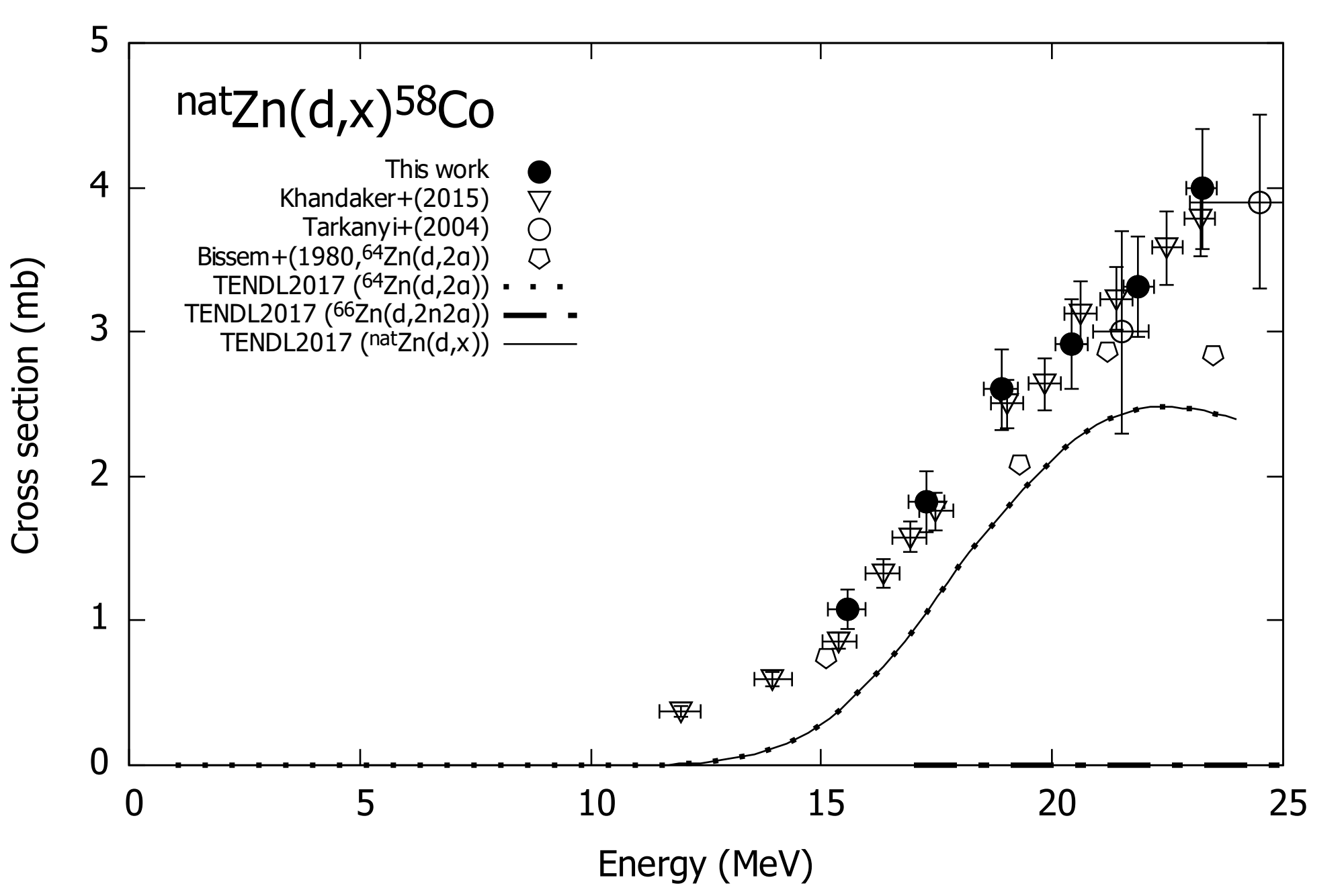
natZn(d,x)58Co
This work
Khandaker+(2015)
Tarkanyi+(2004)
Bissem+(1980,64Zn(d,2α))
TENDL2017 (64Zn(d,2α))
TENDL2017 (66Zn(d,2n2α))
TENDL2017 (natZn(d,x))
Cross section (mb)
Energy (MeV)
0
1
2
3
4
5
0
5
10
15
20
25

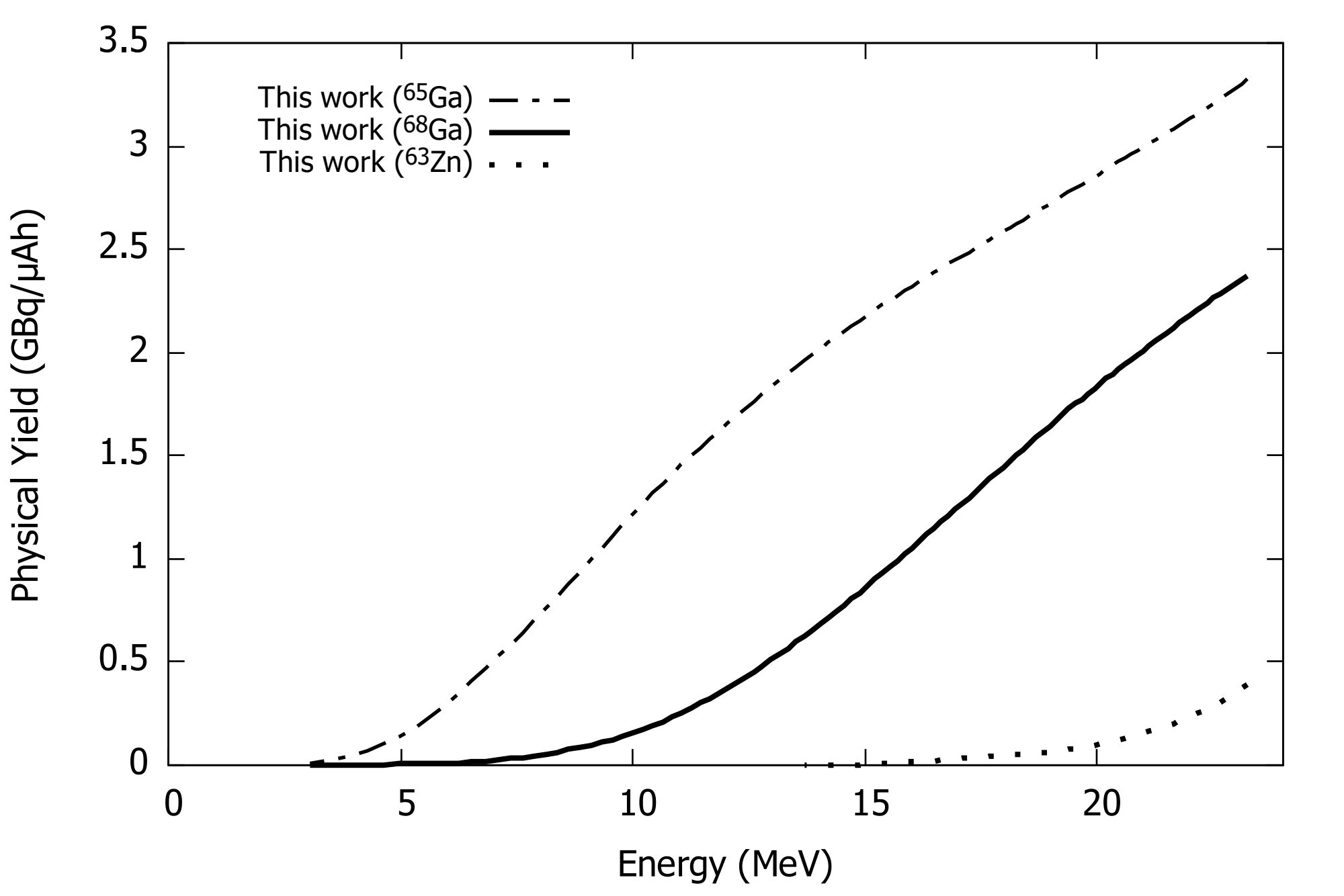
This work (^{65}Ga)
This work (^{68}Ga)
This work (^{63}Zn)
Physical Yield (GBq/μAh)
Energy (MeV)
0
0.5
1
1.5
2
2.5
3
3.5
0
5
10
15
20

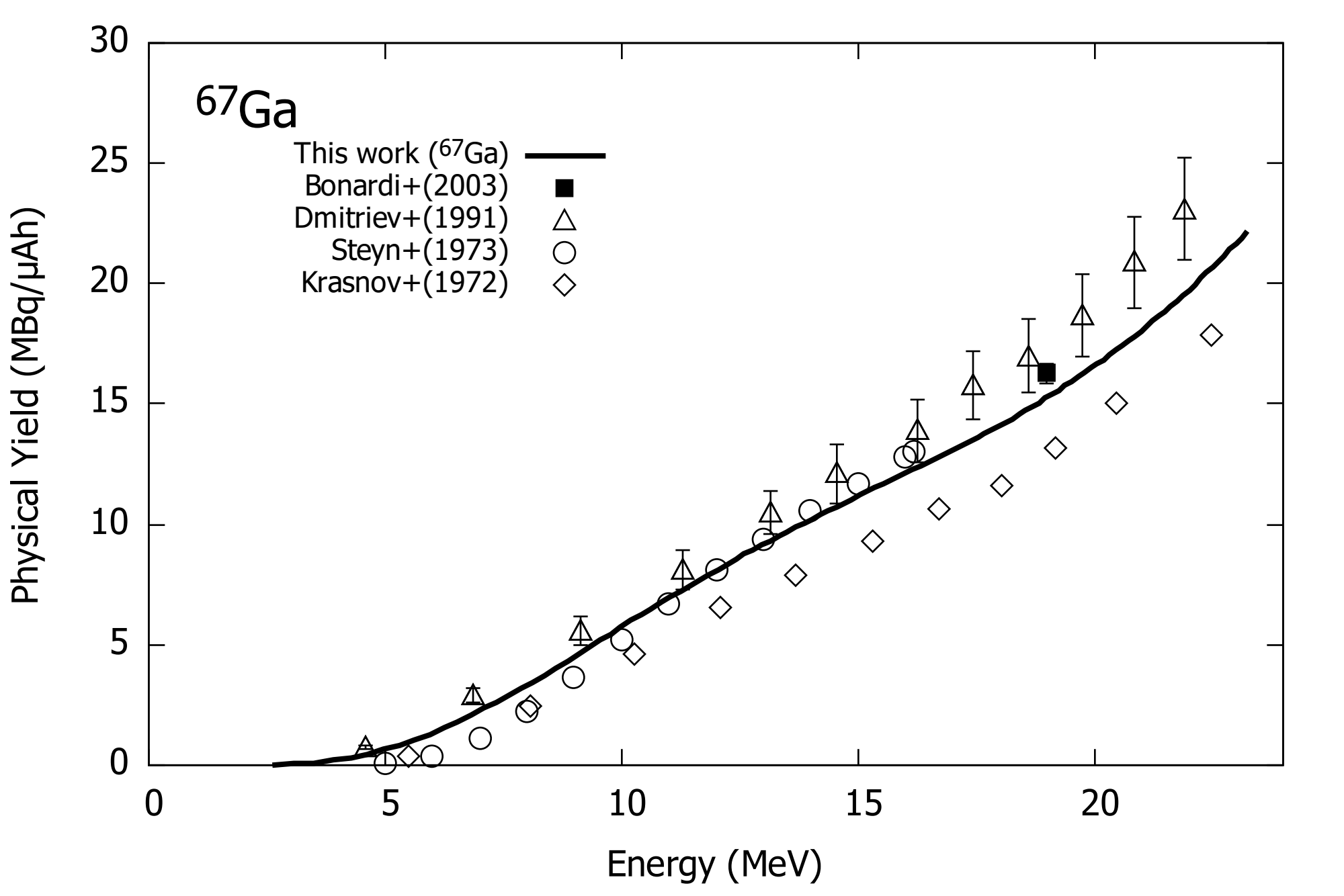
67Ga
This work (67Ga)
Bonardi+(2003)
Dmitriev+(1991)
Steyn+(1973)
Krasnov+(1972)
Physical Yield (MBq/μAh)
Energy (MeV)
0
5
10
15
20
25
30

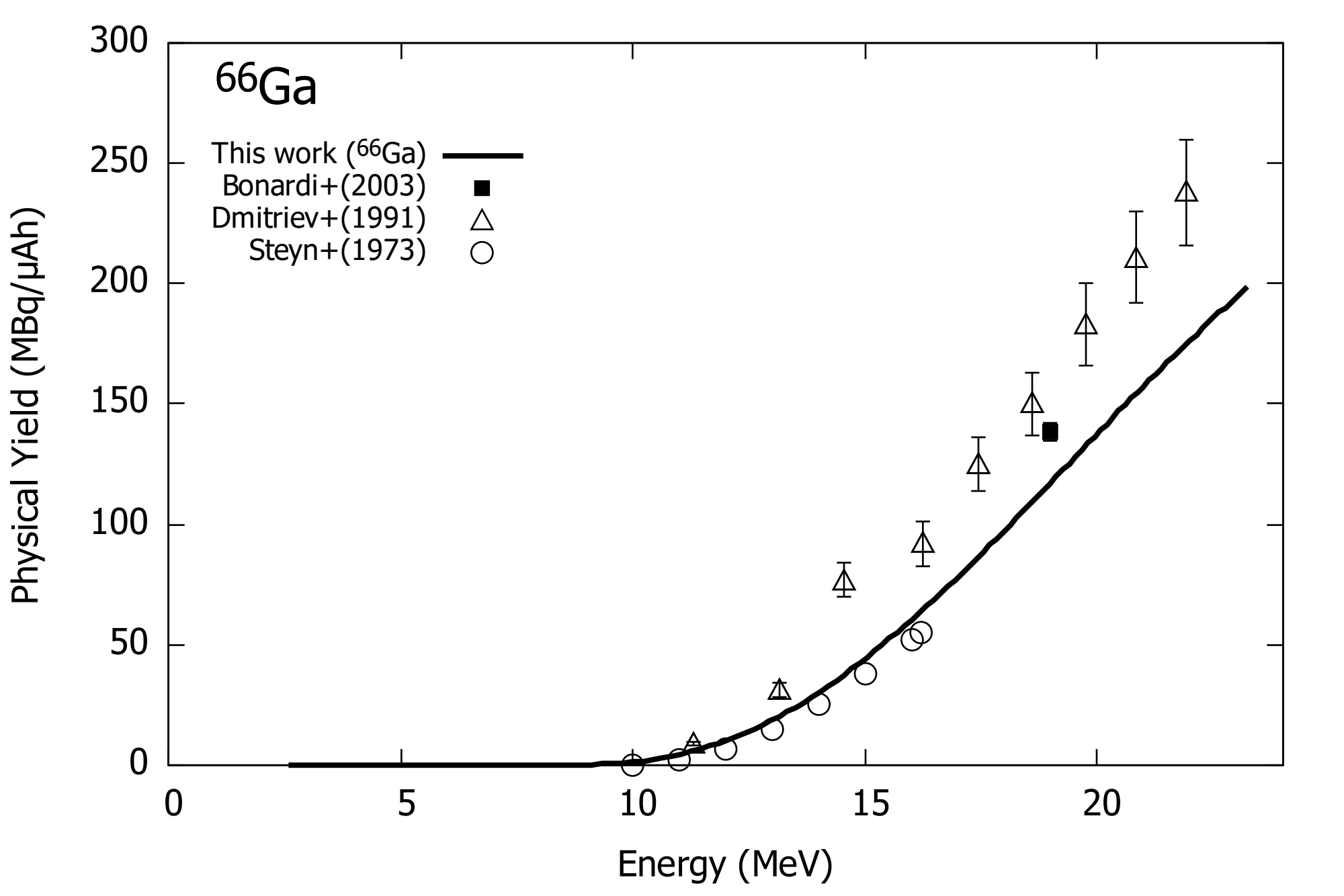
^{66}Ga
This work (^{66}Ga)
Bonardi+(2003)
Dmitriev+(1991)
Steyn+(1973)
Physical Yield (MBq/μAh)
Energy (MeV)
0
50
100
150
200
250
300
0
5
10
15
20

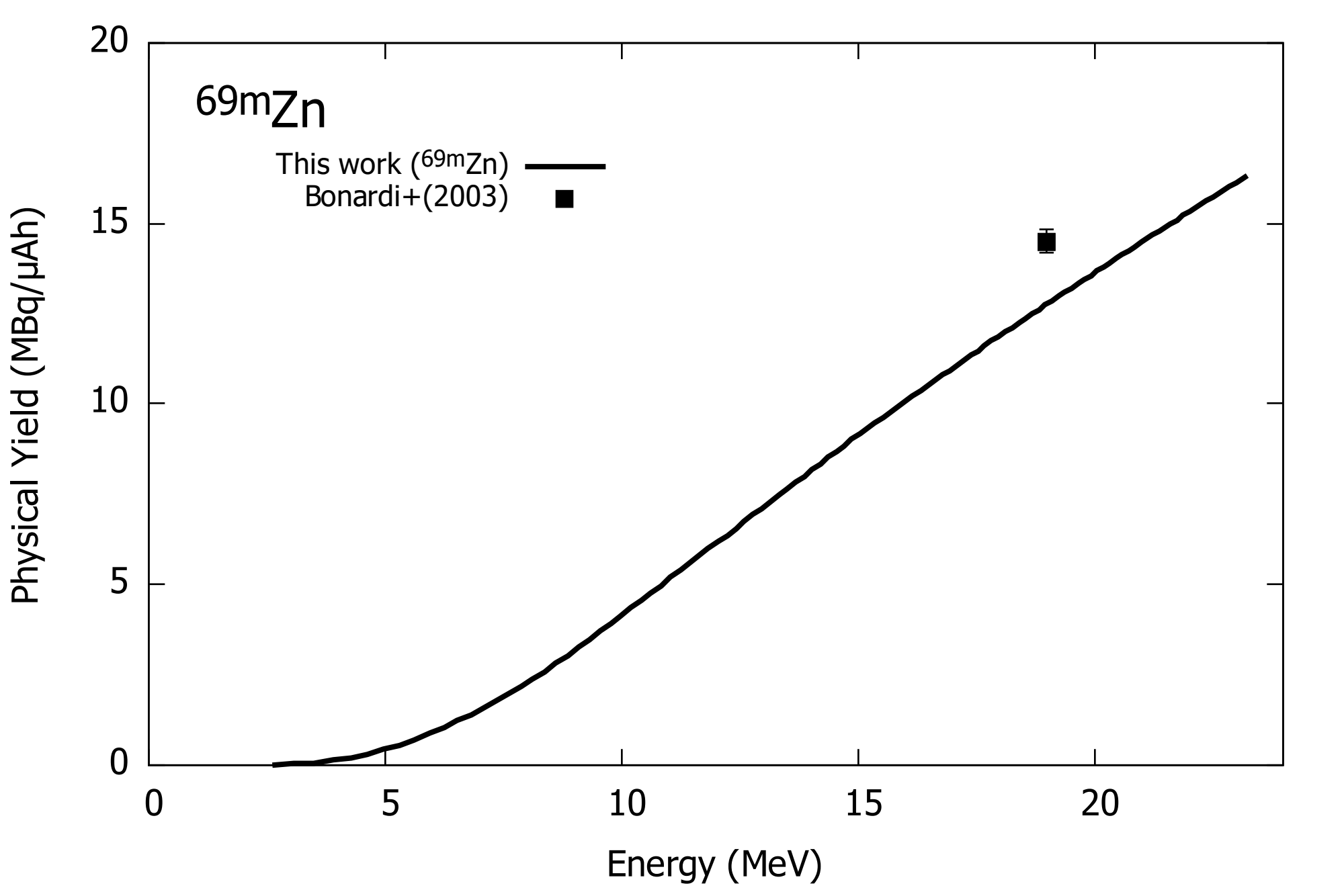
69mZn
This work (69mZn)
Bonardi+(2003)
Physical Yield (MBq/μAh)
Energy (MeV)
0
5
10
15
20

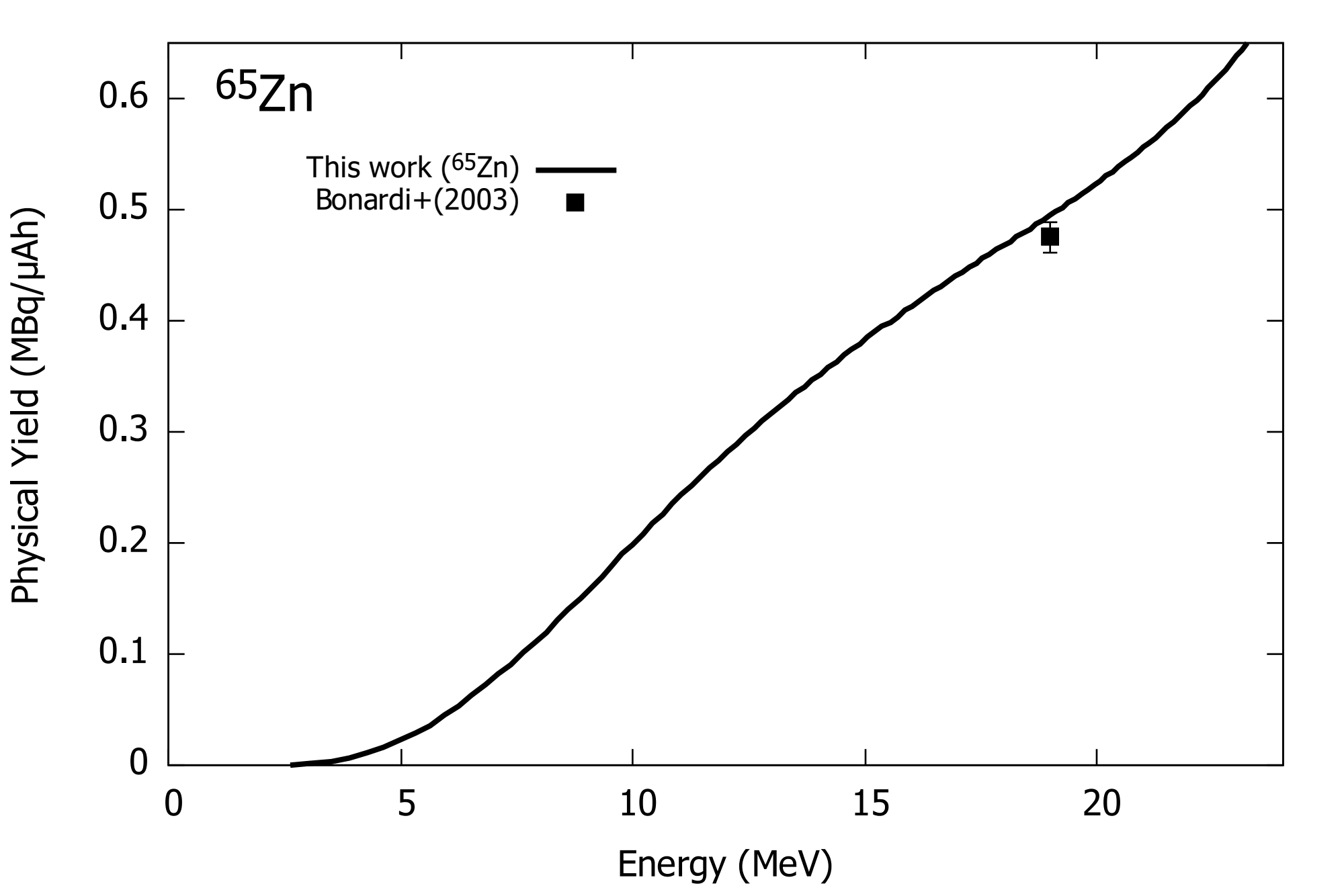
^{65}Zn
This work (^{65}Zn)
Bonardi+(2003)
Physical Yield (MBq/μAh)
Energy (MeV)
0
0.1
0.2
0.3
0.4
0.5
0.6
0
5
10
15
20

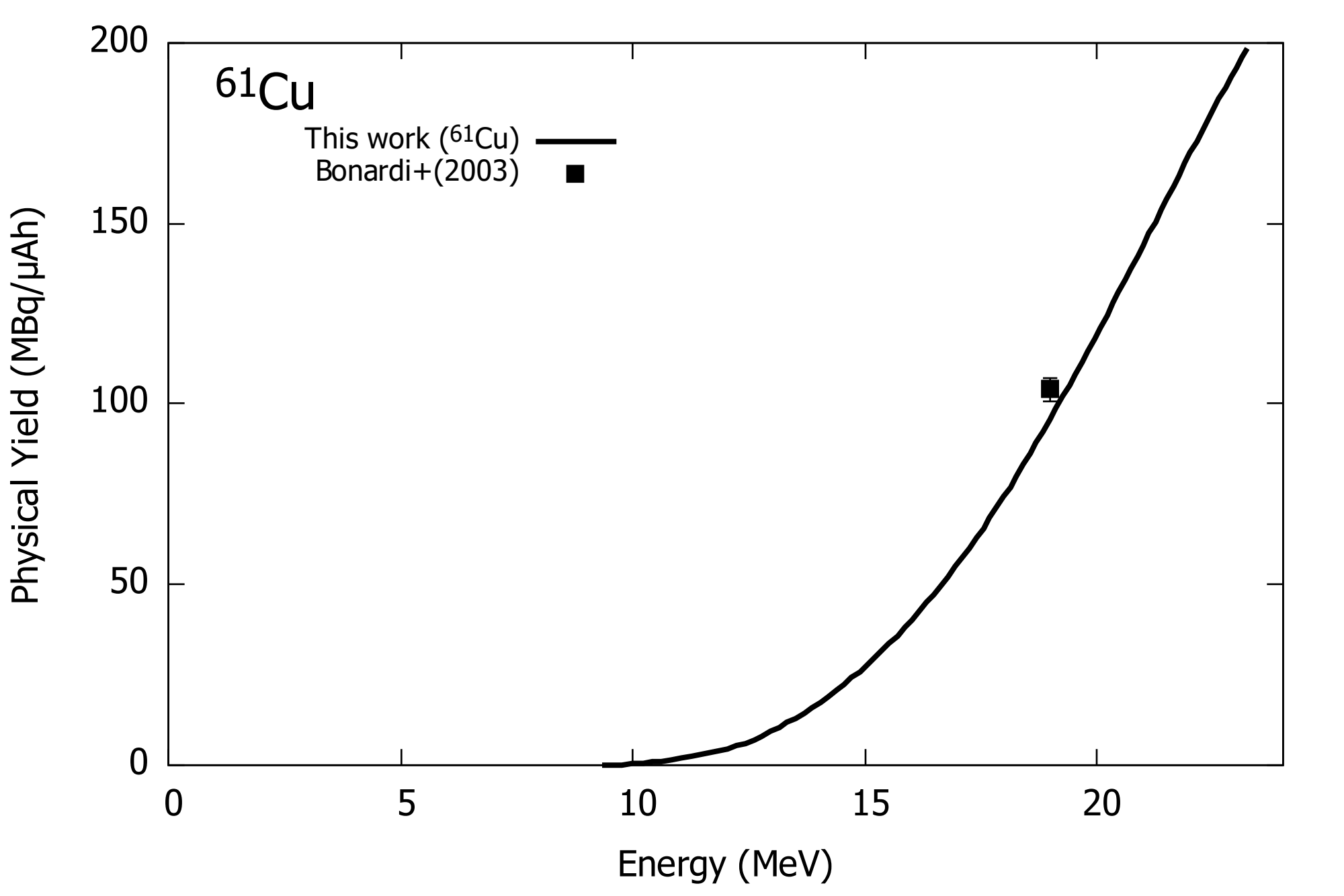
^{61}Cu
This work (^{61}Cu)
Bonardi+(2003)
Physical Yield (MBq/μAh)
Energy (MeV)
0
50
100
150
200
0
5
10
15
20

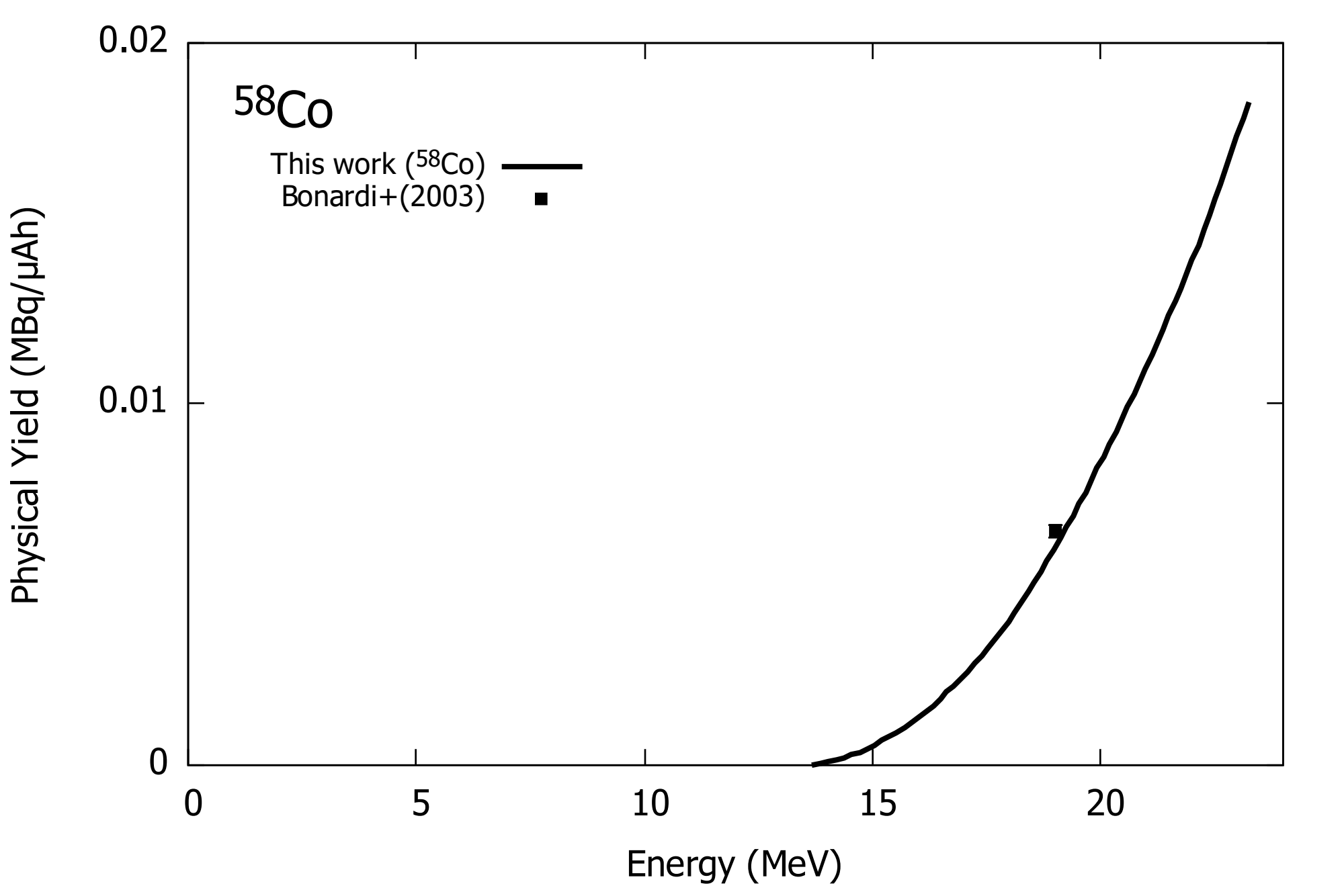
^{58}Co
This work (^{58}Co)
Bonardi+(2003)
Physical Yield (MBq/μAh)
0.02
0.01
0
0
5
10
15
20
Energy (MeV)